# Antiplasmodial 2-thiophenoxy-3-trichloromethyl quinoxalines target the apicoplast of Plasmodium falciparum

Dyhia Amrane, Nicolas Primas, Christophe-Sébastien Arnold, Sébastien Hutter, Béatrice Louis, Julen Sanz-Serrano, Amaya Azqueta, Nadia Amanzougaghene, Shahin Tajeri, Dominique Mazier, et al.

# Antiplasmodial 2-Thiophenoxy-3-trichloromethyl quinoxalines target the apicoplast of *Plasmodium falciparum*.

**Dyhia Amrane[1], Nicolas Primas[1,2]*, Christophe-Sébastien Arnold[3], Sébastien Hutter[4], Béatrice Louis[1], Julen Sanz-Serrano[5], Amaya Azqueta[5,6], Nadia Amanzougaghene[7], Shahin Tajeri[7], Dominique Mazier[7], Pierre Verhaeghe[8,9], Nadine Azas[4], Cyrille Botté[3,*]and Patrice Vanelle[1,2]***

Dedicated to the memory of Professor José Maldonado, PharmD-PhD (1940 – 2020)

[1] Aix Marseille Univ, CNRS, ICR UMR 7273, Equipe Pharmaco-Chimie Radicalaire, Faculté de Pharmacie, 13385 Marseille cedex 05, France
[2] APHM, Hôpital Conception, Service Central de la Qualité et de l'Information Pharmaceutiques, 13005 Marseille, France
[3] ApicoLipid Team, Institute for Advanced Biosciences, Université Grenoble Alpes, La Tronche, France.
[4] Aix Marseille Univ, IHU Méditerranée Infection, UMR VITROME, IRD, SSA, Mycology & Tropical Eucaryotic pathogens, 13005 Marseille cedex 05, France
[5] Department of Pharmacology and Toxicology, Faculty of Pharmacy and Nutrition, University of Navarra, C/ Irunlarrea 1, CP 31008, Pamplona, Navarra, Spain
[6] Navarra Institute for Health Research, IdiSNA, Irunlarrea 3, 31008 Pamplona, Spain
[7] Sorbonne Université, INSERM, CNRS, Centre d'Immunologie et des Maladies Infectieuses, CIMI, 75013 Paris, France
[8] LCC-CNRS Université de Toulouse, CNRS, UPS, 31400 Toulouse, France
[9] CHU de Toulouse, Service Pharmacie, 330 avenue de Grande-Bretagne, 31059 Toulouse cedex 9, France
* Correspondance: nicolas.primas@univ-amu.fr (N.P.); cyrille.botte@univ-grenoble-alpes.fr (C.B.); Patrice.vanelle@univ-amu.fr (P.V)

**Abstract**

The identification of a plant-like Achille's Heel relict, i.e. the apicoplast, that is essential for *Plasmodium* spp., the causative agent of malaria lead to an attractive drug target for new antimalarials with original mechanism of action. Although it is not photosynthetic, the apicoplast retains several anabolic pathways that are indispensable for the parasite. Based on previously identified antiplasmodial hit-molecules belonging to the 2-trichloromethylquinazoline and 3-trichloromethylquinoxaline series, we report herein an antiplasmodial Structure-Activity Relationships (SAR) study at position two of the quinoxaline ring of 16 newly synthesized compounds. Evaluation of their activity toward the multi-resistant K1 *Plasmodium falciparum* strain and cytotoxicity on the human hepatocyte HepG2 cell line revealed a hit compound (**3k**) with a *Pf*K1 $EC_{50}$ value of 0.3 µM and a HepG2 $CC_{50}$ value of 56.0 µM (selectivity index = 175). Moreover, hit-compound **3k** was not cytotoxic on VERO or CHO cell lines and was not genotoxic in the *in vitro* comet assay. Activity cliffs were observed when the trichloromethyl group was replaced by $CH_3$, $CF_3$ or H, showing that this group played a key role in the antiplasmodial activity. Biological investigations performed to determine the target and mechanism of action of the compound **3k** strongly suggest that the apicoplast is the putative target as showed by severe alteration of apicoplaste biogenesis and delayed death response. Considering that there are very few molecules that affect the

*Plasmodium* apicoplast, our work provides, for the first time, evidence of the biological target of trichloromethylated derivatives.

**Key words**
Quinoxaline
Trichloromethyl goup
Plasmodium falciparum
In vitro antiplasmodial activity
Structure-activity relationships
Apicoplast

**Highlights**

- 16 new compounds were obtained in the 2-thiophenoxy-3-trichloromethylquinoxaline series
- **3k** showed good and selective antiplasmodial activity and was not genotoxic
- The trichloromethyl group is essential for providing the antiplasmodial activity
- The hit molecule **3k** showed typical anti-apicoplast activity
- Size of schizonts were affected at high concentration of **3k** without hepatotoxicity

*Graphical abstract*

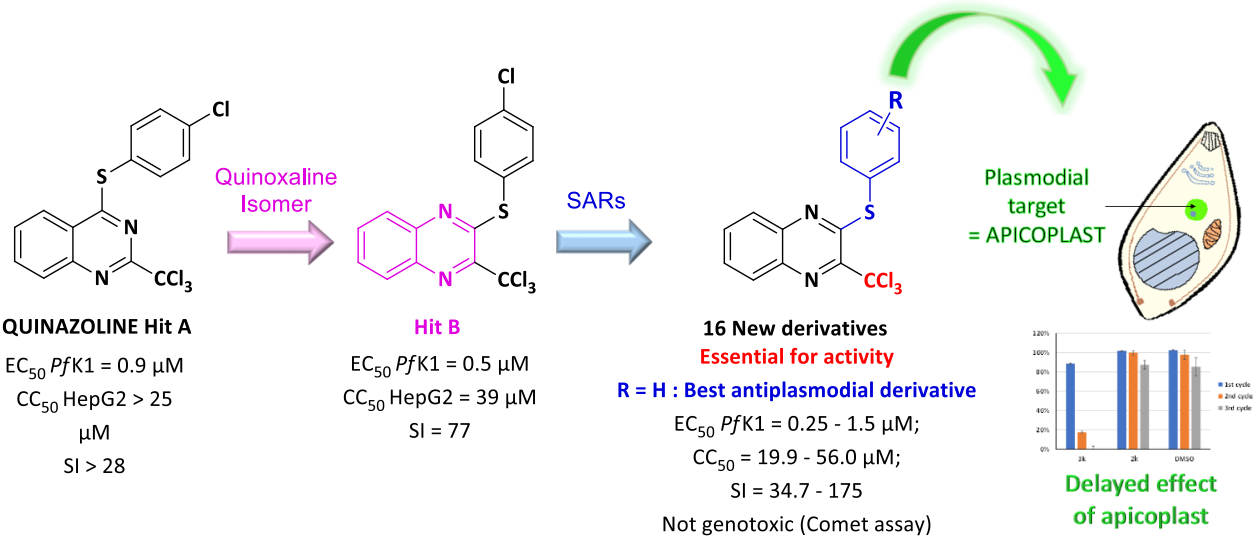


## Introduction

Malaria remains the leading cause of death among parasitic infections worldwide, mainly affecting children under the age of 8, the elderlies and pregnant women. According to the World Malaria Report 2020 [1], malaria caused an estimated 229 million clinical cases leading to 409 000 deaths. Eighty nine countries from the sub-tropical zone are endemic, where the mosquito vectors are present. Most cases and deaths occur in sub-Saharan Africa and South-East Asia. Malaria is caused by a unicellular eukaryote, i.e. protist, of the Apicomplexa phylum and the *Plasmodium* genus, among which the species *falciparum* is responsible for most fatal malaria cases, including cerebral malaria. The parasite is transmitted to humans by a bite of an infected female *Anopheles* mosquito during a blood meal. Despite numerous and ambitious malaria control efforts, *Plasmodium*

strains that resist commercial anti-malarial drugs such as chloroquine [2], quinine [3], atovaquone [4], mefloquine [5], piperaquine [6] and associations of pyrimethamine-cycloguanil [7] or sulfadoxine-pyrimethamine [8] are spreading worldwide. In addition, the emergence of resistances toward the first line treatments against severe *P. falciparum* infections, Artemisinin-based Combination Therapies (ACTs), is now threatening the efficacy of malaria treatment particularly in the Greater Mekong Subregion [9], Africa [10,11] and India [12]. Therefore, new chemotypes with original modes of action, for use in combination therapies, are urgently needed to overcome these resistances and move towards malaria eradication.

Working on the synthesis and reactivity of new heterocycles bearing a trichloromethyl group as potential antiparasitic agents [13-15], our research group has previously reported an antiplasmodial 2-trichloromethylquinazoline derivative (Hit A, Table 1) bearing a thiophenoxy group at position 4 [16]. From this initial compound, a quinoxaline position isomer (Hit B, **Table 1**) was prepared and evaluated, showing an improved antiplasmodial profile [17]. Based on this encouraging result, we decided to synthesize a series of original quinoxaline derivatives bearing a thiophenoxy moiety at the 2-position of the quinoxaline ring, with the aim of identifying a new optimized hit-compound and investigating the antiplasmodial structure-activity relationships.

**Table 1.**

Comparison between antiplasmodial Hit A and position isomer Hit B

| | 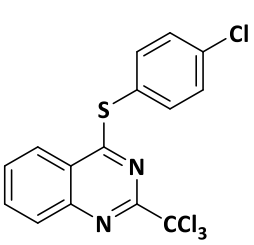 | 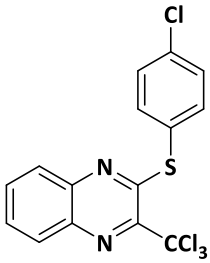 |
|---|---|---|
| | **Hit A** | **Hit B** |
| $EC_{50}$ *Pf*K1 (µM) | 0.9 | 0.5 |
| $CC_{50}$ HepG2 (µM) | >25 | 38.6 |
| Selectivity index (SI) | >28 | 77.2 |

Indeed, several quinoxalines have already been identified as promising antiplasmodial molecules, including BQR695 (**Figure 1**), identified from a phenotypic screening of the Novartis chemical library, exerting antiplasmodial activity through inhibition of the plasmodial protein kinase P*f*PI(4)K [18]. Guillon et *al.* [19] previously described a series of bis- and tris-pyrrolo[*1,2-a*]quinoxaline derivatives (**C**, Figure 1) showing good antiplasmodial activity during the intraerythrocytic stage of *P. falciparum* W2 and 3D7 with $EC_{50}$ in the micromolar range. In addition, (*R*)-enantiomers of pyrrolo[1,2-*a*]quinoxalines (**D**) showed good antiplasmodial activities [20]. In addition, our lab has previously described 2-trichloromethylpyrroloquinoxaline derivatives (**E**) which also show selective antiplasmodial activity [21], illustrating the potential of quinoxaline ring in antiplasmodial drug-design.

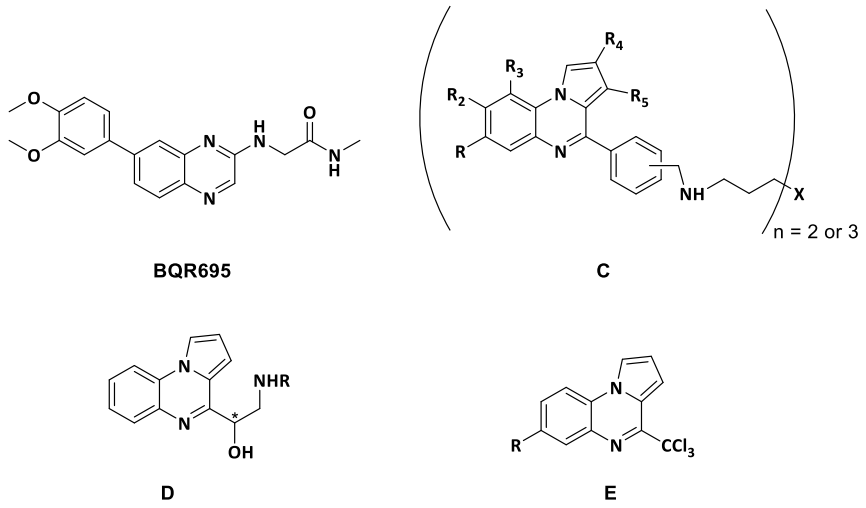


**Figure 1.** Structures of some previously described antiplasmodial derivatives containing a quinoxaline moiety.

With the aim of discovering and developing new antimalarial compounds, Medicines for Malaria Ventures (MMV) defined target candidates (TCPs) and target product profiles (TPPs) for the treatment and chemoprevention of malaria [22]. MMV currently lists four molecules in pre-clinical trials and 14 compounds in clinical trials [23]. Therefore, new compounds with novel mechanisms of action are urgently required to overcome the resistance of *Plasmodium* against commercial drugs. In this context, apicoplast, a plant plastid-like organelle that is essential for parasite survival provide potentially an interesting antimalarial target.

The discovery in Australian corals of a photosynthetic apicomplexan *Chromera veli*a confirmed the common plant and photosynthetic evolutionary origin of *P. falciparum* and its peculiar organelle, the apicoplast [24]. Indeed, the apicoplast is a non-photosynthetic plastid acquired by secondary endosymbiosis from a plastid-containing red algal ancestor [25]. As a consequence of this secondary endosymbiotic origin, the apicoplast is delimited by four membranes [26]. This *P. falciparum* organelle possesses a housekeeping machinery maintained in its small 35 kb circular genome, which encodes for tRNAs, ribosomal proteins and a handful of proteins that are targeted to the apicoplast [27]. Despite being non photosynthetic, the apicoplast retains several anabolic pathways that are essential for parasite survival. These pathways include fatty acids biosynthesis, isoprenoid biosynthesis precursors, iron-sulfur cluster assembly and heme biosynthesis [27]. These metabolic pathways have no equivalent in the human host. Isoprenoid precursors such as isopentenyl pyrophosphate (IPP) have previously been described as the only required function of the apicoplast in the asexual blood stage of malaria parasite *in vitro* under rich culture conditions [28]. Thus, it was confirmed that IPP inhibitors, such as fosmidomycin, mainly target the apicoplast. On the other hand, the apicoplast fatty acid biosynthesis plays a vital role during the *in vitro* liver stage [29], and can be reactivated during the blood stages and become critical in a low host nutritional/lipid environment [30, 31]. Furthermore, even if disrupted and absent in blood stage parasites by anti-plastidial treatment (azythromycin, doxycycline, fosmidomycin), the apicoplast remains metabolically active in the form of vesicles, showing once again that the IPP pathway is not the only essential pathway of the apicoplast [32]. Moreover, Prigge et al. [33] have recently demonstrated the importance of carbon metabolism in the apicoplast of the malaria parasite. Indeed, a loss of pyruvate

kinase II activity which is an essential *Plasmodium* enzyme providing the pyruvate necessary for the generation of essential isoprenoid precursors, leads to a reduction of apicoplast RNA, following by apicoplast disruption and parasite death. Seven enzymes of the isoprenoid precursors pathway are drug-target in the apicoplast, which are DOXP synthase, IspC, IspD, IspE, IspF, IspG and IspH. Knowing that the isoprenoid precursors biosynthesis is localized only to apicoplast, chemical rescue by adding IPP to the growth medium identified **MMV-08138** as a potent IspD inhibitor during the blood stage of *P. falciparum* with an $EC_{50}$ of 110 nM (Figure 2) [34].

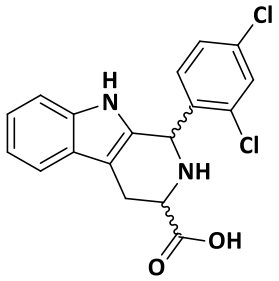


**Figure 2.** MMV-08138 acting at the level of the *Plasmodium* apicoplast.

Currently very few molecules targeting the apicoplast have been reported, but some known antibiotics have been studied, such as ciprofloxacin and doxycycline belonging to the fluoroquinolone and tetracycline classes respectively, which target DNA replication and rRNA translation respectively in *P. falciparum* apicoplast, leading to a delayed death drug-response [26].

The delayed death phenomenon in the apicomplexan parasite is well studied and its molecular mechanism appears to be related to the inhibition of functions in the apicoplast that induce death of daughter cell after one life cycle. It is related to apicoplast housekeeping processes such as DNA replication, transcription and translation mechanisms [27].

In addition to these antibiotics, several biocides such as triclosan (Figure 3) are reported to be active against *Plasmodium* through the metabolic pathway of fatty acid synthesis located in the apicoplast [26] although it was further proved that the apicoplast is not the main target [35]. As *P. falciparum* apicoplast is an essential chloroplast-like organelle, studies have demonstrated that herbicides active against plants are also active against *P. falciparum* and therefore could act as antimalarials [36,37]. Indeed, clomazone [38] and fluridone [39] affect DOXP synthase and block plastidial abscisic acid synthesized by the plastid DOXP pathway respectively, localized in the apicoplast (**Figure 3**).

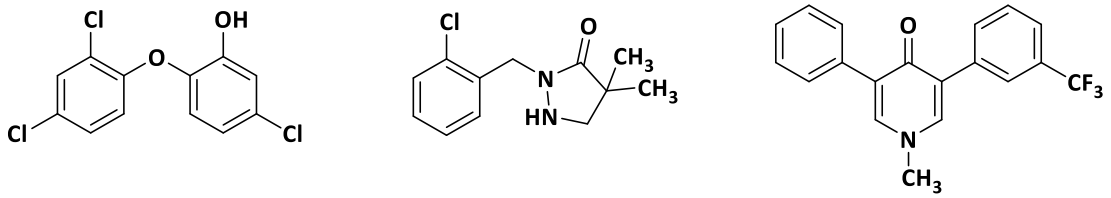


**Triclosan**
**$EC_{50}$ *Pf*3D7 = 1.55 µM**

**Clomazone**

**Fluridone**

**Figure 3.** Chemical structures of antiapicomplexe biocids.

After working for 15 years on the development of trichloromethylated heterocycles without identifying their mechanism of action, we decided herein to evaluate the effect of our molecules

toward this vital organelle in *P. falciparum* in order to look for the mechanism of action of such trichloromethyl derivatives.

## 1. Results

### 1.1. Synthesis

As shown in **Scheme 1**, the key substrate (**1**) was easily obtained by reacting *o*-phenylenediamine with ethyl pyruvate to provide the corresponding lactam which was then chlorinated using $POCl_3$ (Scheme 1) [15]. Next, chlorimine (**1**) was reacted through a nucleophilic aromatic substitution reaction ($S_NAr$) with various thiophenol derivatives in the presence of cesium carbonate in DMF at 70 °C. The desired intermediates (**2a-2p**) were obtained in low to quantitative yields (14 to 100%). Yield variation does not seem to be correlated with the electron-donating or -withdrawing behavior of the different thiophenol substituents. Finally, from the methylated precursors (**2a-2p**), a chlorination reaction using $PCl_5$ and $POCl_3$ was performed under microwave heating at 100 °C for 30 min, according to a previously reported method [40], leading to the target compounds (**3a-3p**) in low to very good yields (15-86%). A series of 16 original derivatives (**3a-3p**) was then prepared, bearing electron-donating or electron-withdrawing substituents in *ortho*, *meta* and *para* positions of the thiophenol moiety. It is to note that attempt to chlorinate the intermediate (**2i**), bearing a 3'-OMe substituent on the thiophenoxy group, led to the only the unexpected 2'-chlorinated product.

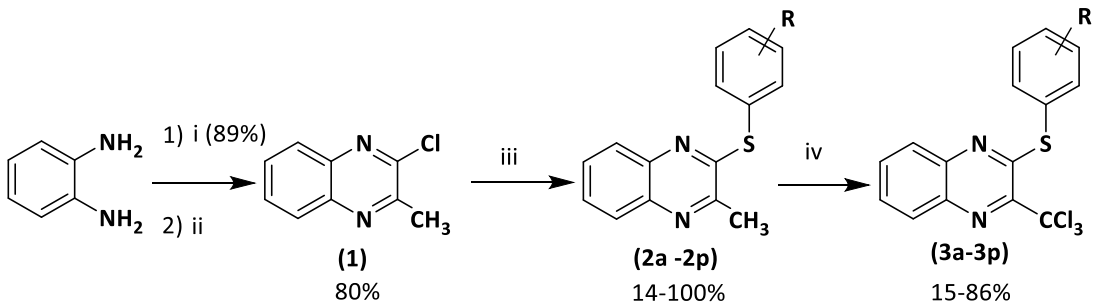


**Scheme 1.** Preparation of 2-thiophenoxy-3-trichloromethylquinoxaline derivatives (**3a-3p**). *Reagents and conditions*: (i) ethyl pyruvate 1 equiv, $H_2O$, 50 °C, 15 min; (ii) $POCl_3$, reflux, 2 h; (iii) appropriate thiophenol derivative 1 equiv, $Cs_2CO_3$ 1 equiv, anh. DMF, 70 °C, 12 h, sealed vial, $N_2$; (iv) $PCl_5$ 6 equiv, $POCl_3$ as solvent, 100 °C, MW, 20 min, 800 W.

### 1.2. Biological results

*Structure-Activity Relationship (SAR*) study

These new derivatives were evaluated *in vitro* against the K1 multidrug-resistant *P. falciparum* strain, by determining their 50% efficacy concentration ($EC_{50}$), and compared with three reference antimalarial drugs: chloroquine, atovaquone and doxycycline. The *in vitro* 50% cytotoxic concentrations ($CC_{50}$) were assessed on the HepG2 human hepatocyte cell line and compared with cytotoxic reference drug: doxorubicin. Selectivity indexes were calculated: SI = $CC_{50}/EC_{50}$. The results are presented in **Table 2**.

All the 16 newly synthesized compounds showed good aqueous solubility except for compound (**3j**), which precipitated above 1.9 µM in the cell viability assay. The derivatives showed cytotoxicity values ranging from 19.9 to 69.7 µM, comparable or better than chloroquine (30 µM) or doxycyclin (20 µM). It appears that strong electron-withdrawing groups (EWG) (**3m-3o**) at 4-position

of 2-thiophenoxy group led to slightly more cytotoxic compounds (19.9-29.9 µM), contrary to electron-donating groups (EDG) (**3p**) or the unsubstituted thiophenoxy moiety (**3k**) (69.7-56.0 µM, respectively).

With regard to the antiplasmodial activity, all derivatives showed submicromolar activity except for (**3p**) bearing a 4-Me group (1.5 µM). A strong EWG such as 4-$NO_2$ group (**3o**) gave the best antiplasmodial activity with only 0.2 µM. The 2, 3 or 4 fluoro-substituted thiophenoxy moiety (**3e-3g**) led to quite similar activities (0.32, 0.31, 0.36 µM respectively). Other 4-EWG such as 4-$CF_3$ (**3m**) and 4-$OCF_3$ (**3n**) gave quite similar activities to the fluoro-substitued thiophenoxy group (0.40 and 0.30 µM respectively). Substitution by a methoxy group was slightly detrimental to the activity, especially for the 2-OMe compound (**3h**) (0.74 µM). The disubstituted 2-chloro-3-methoxy-thiophenoxy moiety (**3i**) led to a better antiplasmodial activity than only 2- or 4-methoxy substitution (**3h**, **3j**). For the dichloro-containing molecules (**3c, 3d**), 2-3 substitutions were better than the 2-4 substitutions (0.31 vs 0.90 µM).

Finally, the best compound in this series was the unsubstituted thiophenoxy group (**3k**) which combined both good antiplasmodial activity and low cytotoxicity, leading to the highest selectivity index in the series (175) (**Table 2**). It is to note that there is no correlation between the calculated logP and activity.

**Table 2.** Antiplasmodial activity, cLogP and human cell toxicity on HepG2 cell line of the 2-phenoxy-3-trichloro-methylquinoxaline compounds (**3a-3p**).

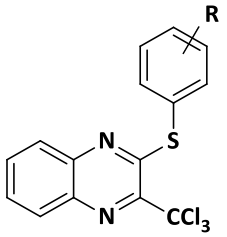


| R | N° | Yields (%) | $EC_{50}$ P*f*K1 (µM) | $CC_{50}$ HepG2 (µM) | SI[d] | cLogP[e] |
|---|---|---|---|---|---|---|
| **2-Cl** | 3a | 62 | 0.50 ± 0.10 | 36.9 ± 8.1 | 73.8 | 5.15 |
| **3-Cl** | 3b | 74 | 0.41 ± 0.08 | 38.3 ± 8.1 | 93.4 | 5.16 |
| **2,3-Cl** | 3c | 61 | 0.31 ± 0.06 | 34.6 ± 7.1 | 111.6 | 5.68 |
| **2,4-Cl** | 3d | 46 | 0.90 ± 0.10 | >31.2[c] | >34.7 | 5.69 |
| **2-F** | 3e | 56 | 0.32 ± 0.07 | 40.5 ± 8.1 | 126.6 | 4.94 |
| **3-F** | 3f | 63 | 0.31 ± 0.07 | 35.9 ± 7.9 | 115.8 | 4.94 |
| **4-F** | 3g | 51 | 0.36 ± 0.08 | 30.8 ± 7.0 | 85.6 | 4.95 |
| **2-OMe** | 3h | 64 | 0.74 ± 0.16 | 42.6 ± 5.2 | 56.8 | 4.63 |
| **2-Cl-3-OMe** | 3i | 15 | 0.46 ± 0.15 | 58.4 ± 5.8 | 126.9 | 5.14 |
| **4-OMe** | 3j | 59 | 0.65 ± 0.15 | >1.9[c] | >3.0 | 4.61 |
| **H**[f] | **3k** | **71** | **0.32** ± 0.07 | **56.0** ± 11.0 | **175.0** | **4.68** |
| **4-Br** | 3l | 44 | 0.46 ± 0.10 | 42.2 ± 8.6 | 93.0 | 5.25 |
| **4-$CF_3$** | 3m | 80 | 0.50 ± 0.10 | 29.9 ± 5.1 | 59.8 | 5.68 |
| **4-$OCF_3$** | 3n | 68 | 0.36 ± 0.10 | 21.0 ± 3.1 | 58.3 | 5.55 |
| **4-$NO_2$** | 3o | 64 | 0.25 ± 0.05 | 19.9 ± 3.0 | 79.6 | 3.92 |

| | | | | | | |
|---|---|---|---|---|---|---|
| **4-$CH_3$** | 3p | 40 | 1.50 ± 0.20 | 69.7 ± 14.6 | 46.5 | 5.01 |
| **Hit B** | | | 0.50 | 38.6 | 77.2 | 5.17 |
| **Chloroquine[a]** | | | 0.80 | 30.0 | 37.5 | 3.82 |
| **Atovaquone[a]** | | | 0.001 | >15.6 | 15600 | 4.23 |
| **Doxycycline[a]** | | | 6.00 | 20.0 | 3.3 | - |
| **Doxorubicin[b]** | | | - | 0.20 | - | - |

[a] Chloroquine, Atovaquone and doxycycline were used as antimalarial reference-drugs; [b] Doxorubicin was used as a cytotoxic reference-drug; [c] Highest concentration tested due to a lack of solubility; [d] Selectivity index (SI) was calculated according to the formula: SI = $CC_{50}/EC_{50}$, [e] Weighted clogP was computed by swissADME; [f] The best antiplasmodial molecule.

*Toxicity data*

In order to complete the cytotoxicity data of the best molecule (**3k**) in this series, we tested it on CHO Chinese Hamster Ovary cells and Vero cells (**Table 3**). After 72 h of treatment, low cytotoxicities was observed both on cell lines (58.5 µM and 63.5 µM respectively), similar to that measured on HepG2 cell line (56.0 µM).

To complete the *in vitro* toxicological evaluation of compound (**3k**), its genotoxic potential was studied, using the comet assay on the HepG2 cell line (**Table 3**). Compound (**3k**) did not induce DNA strand breaks or alkali labile sites after either short (2 h) or long (72 h) exposure at two concentrations (5.6 and 28 µM; $CC_{50}/2$ and $CC_{50}/10$ after 72 h of treament) ( see supplementary material). The positive control (i.e., cells treated with 1 mM Methyl MethaneSulphonate, MMS) showed the expected results.

**Table 3.** Cytotoxic and genotoxic data for hit compound (**3k**).

| Entry | $CC_{50}$ HepG2 (µM) | $CC_{50}$ CHO (µM) | $CC_{50}$ Vero (µM) | Comet assay[a] |
|---|---|---|---|---|
| 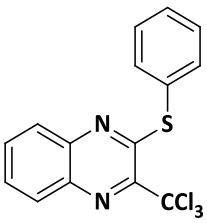 **(3k)** | 56.0 ± 11.0 | 58.5 ± 3.9 | 63.5 ± 8.6 | Negative |

[a] Comet assay was performed on HepG2 cell line at 5.6 and 28 µM for 2 or 72 h.

*Role of the 2-$CCl_3$ group*

We have previously shown that the -$CCl_3$ group is mandatory to provide antiplasmodial activity [17, 21, 41]. To confirm the key role of the $CCl_3$ group in the activity of **3k**, we compared the antiplasmodial activity of (**3k)** with that of three analogs bearing a proton (**3r**), a methyl group (**2k**) or a trifluoromethyl group (**3s**) at position 3 of the quinoxaline ring respectively. None of these analogues lacking a $CCl_3$ group was active against *P. falciparum* ($EC_{50}$ *Pf*K1 > 50 µM). These activity

cliffs revealed once again the key role of the $CCl_3$ group in antiplasmodial activity in the studied series (**Figure 4**) [42].

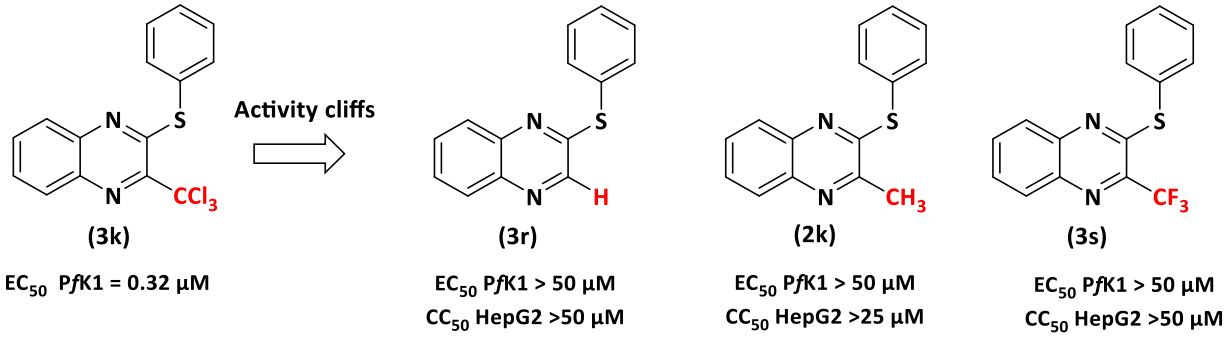


**Figure 4.** Comparison of the *in vitro* antiplasmodial activities of hit molecule **3k** with analogs **3r, 2k** and **3s**.

*Evaluation on P. falciparum apicoplast*

- *Treatment with molecule **3k** affects parasites growth and apicoplast development*

Using an epifluorescence microscope, we monitored the effect of molecule (**3k**) on different intraerythrocytic stages of *P. falciparum* parasite in order to identify the mechanism by which the molecule could affect parasite survival and whether this was directed against the apicoplast. The loss of apicoplast by molecule (**3k**)-treatment can then be visualized via fluorescence microscopy. The $EC_{50}$ treatment was performed on synchronized cultures of *P. falciparum* 3D7 strain during a 48-hour parasite life cycle (**Figure 5A**).

Parasites treated with 0.3 µM of molecule (**3k**) shows a severe defect in apicoplast biogenesis when compared to the DMSO control. The apicoplast development, elongation and branching typically happening during asexual blood stage intracellular development is highly affected by the treatment and strongly suggest a direct effect on *Plasmodium* apicoplast (**Figure 5A**). Furthermore, overall parasite development is also slightly reduced, as the nucleus staining shows a defect in replication and the culture is enriched in mid trophozoite parasites (**Figure 5A**), suggesting either that apicoplast disruption induces parasite death or that the drug could have some sort of off target mechanism. If the apicoplast is the primary target of the (**3k**) molecule, one could expect a so-called delayed death phenotype, which is characteristic of some apicoplast targeting drugs such as chloramphenicol, doxycycline or ciprofloxacin. To confirm this, we performed a growth assay on three life cycles (3x 48 h) by measuring the development of treated parasite with 0.3 µM of (**3k**) and 0.3 µM of (**2k**). The replacement of $CCl_3$ by a methyl group in (**2k**) analog shows to have no effect on the apicoplast development (**Figure 5B**) compared to untreated parasites (DMSO control). Results show a slight reduction of the parasites development at the first cycle (48 h), and a drastic reduction of the growth at the second and third cycles, confirming the delayed effect of apicoplast targeting drugs, compared to inactive (**2k**) molecule, which has no significative difference with DMSO (**Figure 5C**). Nevertheless, the slight decrease of the growth at the first cycle confirms the potential off target of (**3k**) molecule, outside of the apicoplast, coherent with the reduction of nucleus replication shown by IFA at 48 h treatment (**Figure 5A**).

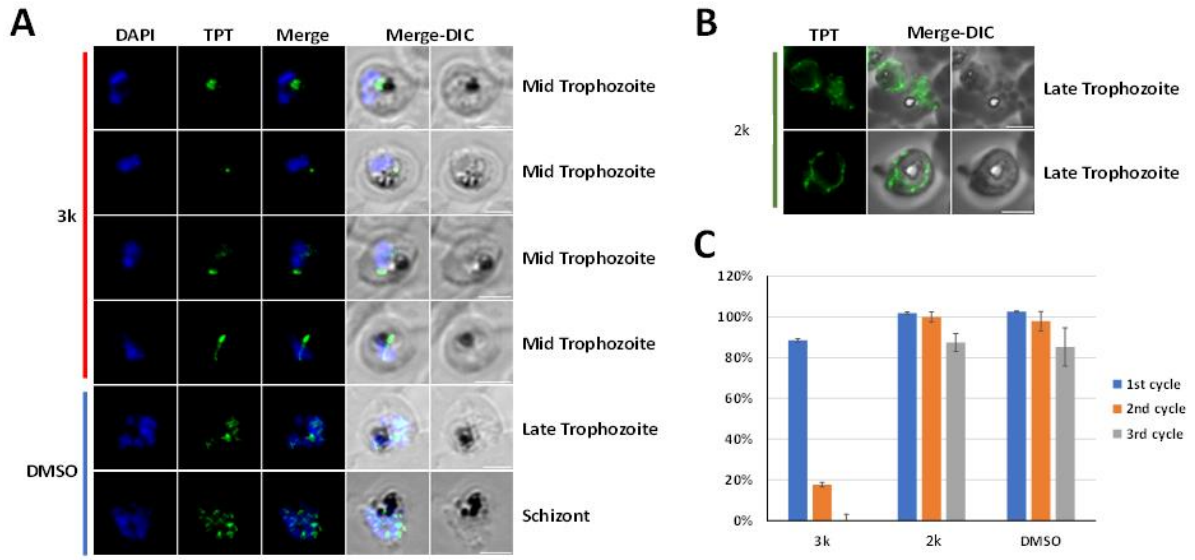


**Figure 5**. (**3k**) molecule treatment affects apicoplast biogenesis.
**(A, B)** Triose Phosphate Transporter (TPT) fluorescent signal is shown in green (TPT labeled with an 3xHA tag). DAPI, as a marker for the nucleus, is shown in blue. Apicoplasts of treated parasites with 0.3 µM of (**3k**) molecule or 0.3 µM of (**2k**) molecule are compared to normal plastid visualized in DMSO-treated control. The microscopic images were obtained by epifluorescence microscope. DIC, differential interference contrast. **(C)** Plastid associated with the delayed death of *P. falciparum* trophozoite was observed after treatment with molecule **(3k)** on three life cycles (n = 3, error bar = standard deviation, SD).

It should be noted out that all derivatives (**3a-p**) including (**3k**) have a high lipophilicity (3.92 < clogP < 5.69). This may be necessary property to cross the four membranes that envelop the apicoplast.

*Evaluation on human hepatocyte infection*

In order to further explore the potency of molecule (**3k**), an evaluation was made on the hepatic stage of *P. falciparum* infection. Cryopreserved primary human hepatocyte cultures were infected with *P. falciparum* NF135 strain. Treatment with (**3k**) at various doses was applied simultaneously with the sporozoites addition to hepatocytes and contact was maintained until post-infection day 6 (pi). (**3k**) treatment significantly reduced parasite size without affecting parasite numbers in a dose-dependent manner. Atovaquone (ATQ), a potent hepatic schizonticide was used as positive control.

We then tried to understand if apicoplast of *P. falciparum* schizonts was targeted by (**3k**). In untreated control wells fixed at day 6 pi, the parasitic apicoplast has a uniform appearance. The apicoplast is in its terminal stage of development (considering the 5-6 days schizogony of *P. falciparum*) and the Apicoplast protein acyl Carrier Protein (ACP) signal looks like small dots densely decorating the periphery of the organelle. In (**3k**) treated cultures, the integrity of small dots shown in the control parasites appears to be affected and the ACP signal is condensed leading to the appearance of larger aggregates. At the high dose of 30 µM approximatively 93% of *P. falciparum* schizonts showed partial or complete alteration of the apicoplast signal (**Figure 6**). Interestingly, no cytotoxicity was observed on human hepatocytes up to 30 µM (**Figure 7**).

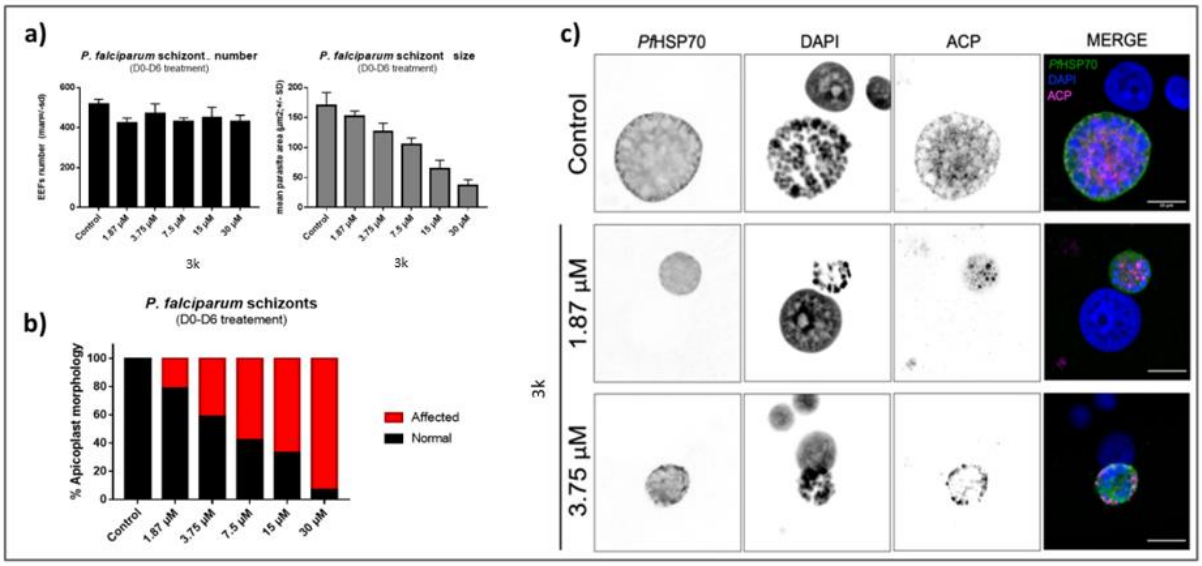


**Figure 6.** The effect of (**3k**) on liver stage *P. falciparum* growth. a) D0 pi-D6 (**3k**) exposure of human hepatocytes infected with *P. falciparum* and its impact on parasite numbers expressed as mean +/- SD and parasite size expressed as surface area expressed as $\mu m^2$ mean +/- SD. Parasites were immunostained with anti-HSP70 antibody and plates were scanned. b) Quantification of different apicoplast morphologies (normal and affected) in 100 parasites with percentage distribution of each defined category. c) Confocal microscopic images of control and treated *P. falciparum* schizonts. The schizonts were immunolabelled with anti-HSP70 antibody. Host and parasite DNA were visualized by 4′,6-diamidino-2-phenylindole (DAPI) dye. The apicoplast was labelled by Anti-PyACP (Scale bar = 10 µm).

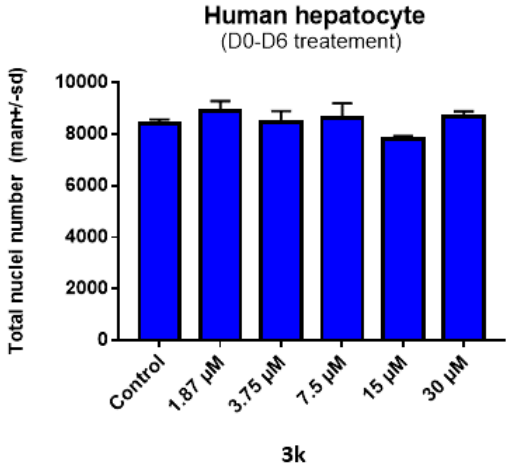


**Figure 7.** Toxicity of (**3k**) on primary human hepatocytes. The number of hepatocyte nuclei quantified from a certain number of microscopic scanning fields from control and (**3k**) treated groups.

## 2. Conclusion

An antiplasmodial SAR study was conducted through the synthesis and evaluation of 16 original thiophenoxyquinoxaline derivatives. All of these molecules displayed good *in vitro* antiplasmodial

activity. Among these compounds, (**3k**) showed the best antiplasmodial activity ($EC_{50}$ = 0.32 µM) and low cytotoxicity towards three cell-lines and no cytotoxicity on human hepatocytes. Moreover, compound (**3k**) presented no genotoxic effect in the comet assay. The activity cliffs showed that the $CCl_3$ group was essential to provide antiplasmodial activity. Although no effect was demonstrated on hepatic stage, at high concentration, the size of parasite was affected. Interestingly, the molecule (**3k**) shows a delayed death inhibition and apicoplast biogenesis branching defect, confirming that it affects growth of *P. falciparum* by targeting the apicoplast, and probably another target outside of the apicoplast which affects the cell division. Essential metabolic pathways reside within the apicoplast which provide promising new drug targets for the development of new antimalarials, with a novel mechanism of action. Further investigations will be necessary in order to decipher the action of trichloromethylquinoxaline derivatives on the apicoplast.

**Acknowledgments**

Funding: This work was supported by the French Agence Nationale de la Recherche [grant number ANR-17-CE11-0017]; the Fondation pour la Recherche Médicale (FRM) [grant number DCM20181039565].

## Experimental section

### 2.1. Chemistry

#### 2.1.1. Generality

Melting points were determined on a Köfler melting point apparatus (Wagner & Munz GmbH, München, Germany) and are uncorrected. Elemental analyses were carried out at the Spectropole, Faculté des Sciences de Saint-Jêrome (Marseille) with a Thermo Finnigan EA1112 analyzer (Thermo Finnigan, San Jose, CA, USA). NMR spectra were recorded on a Bruker AV (Billerica, MA, USA) 200 or AV 250 spectrometers or on a Bruker Avance NEO 400MHz NanoBay spectrometer at the Faculté de Pharmacie of Marseille or on a Bruker Avance III nanobay 400 MHz spectrometer at the Spectropole, Faculté des Sciences de Saint-Jêrome (Marseille). ($^1$H NMR: reference $CDCl_3$ δ = 7.26 ppm, reference DMSO-$d_6$ δ = 2.50 ppm and $^{13}$C NMR: reference $CHCl_3$ δ = 76.9 ppm, reference DMSO-$d_6$ δ = 39.52 ppm). The following adsorbent was used for column chromatography: silica gel 60 (Merck KGaA, Darmstadt, Germany, particle size 0.063–0.200 mm, 70–230 mesh ASTM). TLC was performed on 5 cm × 10 cm aluminum plates coated with silica gel 60F-254 (Merck) in an appropriate eluent. Visualization was performed with ultraviolet light (234 nm). The purity of synthesized compounds was checked by LC/MS analyses, which were performed at the Faculté de Pharmacie of Marseille with a Thermo Scientific Accela High Speed LC System® (Waltham, MA, USA) coupled to a single quadrupole mass spectrometer Thermo MSQ Plus®. The RP-HPLC column is a Thermo Hypersil Gold® 50 × 2.1 mm (C18 bounded), with particles of a diameter of 1.9 mm. The volume of sample injected on the column is 1 µL. The chromatographic analysis with a total duration of 8 min, is performed on the following solvents gradient: t = 0 min, methanol/water 50:50; 0 < t < 4 min, linear increase in the proportion of methanol to a methanol/water ratio of 95:5; 4 < t < 6 min, methanol/water 95:5; 6 < t < 7 min, linear decrease in the proportion of methanol to return to a methanol/water ratio of 50:50; 6 < t< 7 min, methanol/water 50:50. The water used was buffered with ammonium acetate 5 mM. The flow rate of the mobile phase was 0.3 mL/min. The retention times ($t_R$) of the molecules analyzed are indicated in min. The microwave reactions were performed using multimode reactors: ETHOS Synth Lab station and MicroSYNTH® Lab terminal 1024 (Ethos start, MLS GmbH, Leutkirch, Germany.); or monomode reactors: Biotage Initiator® classic in sealed vials with a power output of 0

to 400 W. Reagents were purchased and used without further purifications from Sigma-Aldrich or Fluorochem.

### 3.1.2. 2-Chloro-3-methylquinoxaline (1)

**Step 1**: To a solution of *o*-phenylenediamine (6 g, 1.0 equiv) in $H_2O$ was added ethyl pyruvate (1.0 equiv) dissolved in $H_2O$ (80 mL). The reaction mixture was heated at 50 °C for 15 to 30 min. After cooling, the precipitate product of 3-methylquinoxalin-2(*1H*)-one was recrystallized from ethanol as a white solid, 7.92 g, yield 89%. This was used directly in step 2.

**Step 2**: To a solution of 3-methyl-2(*1H*)-quinoxalinone (12.5 g, 121.8 mmol, 1.0 equiv) was added cold $POCl_3$ (65 mL) in portions to get a slurry. The mixture was refluxed for 2 h. Then, the reaction was added to ice cold water (500 mL) and basified slowly under cooling with $Na_2CO_3$ to pH 8. The organic phase was separated and washed with brine, dried over anhydrous $MgSO_4$, filtered, and concentrated in vacuum to afford the crude product, which was purified by silica gel flash chromatography (using dichloromethane) to afford (**1**) as an off-white solid, yield 80% (7g). Mp 84 °C. **$^1$H NMR (250 MHz, $CDCl_3$)** $\delta$ 8.08 – 7.84 (m, 2H), 7.79 – 7.62 (m, 2H), 2.82 (s, 3H). **$^{13}$C NMR (63 MHz, $CDCl_3$)** $\delta$ 152.9, 147.9, 141.0, 141.0, 130.2, 130.1, 128.5, 128.2, 23.4. Spectral data matched with literature [43].

### 3.1.3. General procedure for 3-methyl-2-substituted-quinoxaline (2a-2p)

To a solution of 2-chloro-3-methylquinoxaline (**1**) (500 mg, 2.8 mmol) and the appropriate thiophenol (2.8 mmol, 1.0 equiv) in anhydrous DMF (10 mL), $Cs_2CO_3$ (912 mg, 2.8 mmol, 1.0 equiv) was added under inert atmosphere. The mixture was stirred at 70 °C overnight. After completion of the reaction, water was added, leading to a precipitate which was separated by filtration. The resulting precipitate was then thoroughly washed with water. The precipitate was dissolved in $CH_2Cl_2$ and dried with $Na_2SO_4$. After filtration and evaporation, the resulting solid was purified by silica gel column chromatography (using the appropriate eluant) to afford the desired compound.

#### 3.1.3.1. 2-(2-Chlorophenylthio)-3-methylquinoxaline (2a)

Yield 100% (803 mg). White solid. Mp 155 °C. **$^1$H NMR (250 MHz, $CDCl_3$)** $\delta$ 7.97 – 7.93 (m, 1H), 7.70 – 7.51 (m, 5H), 7.46 – 7.31 (m, 2H), 2.82 (s, 3H) . **$^{13}$C NMR (63 MHz, $CDCl_3$)** $\delta$ 154.6, 151.5, 141.6, 139.6, 139.6, 137.6, 131.0, 130.4, 129.2, 128.7, 128.3, 128.2, 128.1, 127.5, 22.4. **LC-MS** (ESI+) $t_R$ 6.54 min; m/z $[M+H]^+$ 286.36/289.00. MW: 286.78 g.mol$^{-1}$. **HRMS (ESI)**: m/z calcd. for $C_{15}H_{11}ClN_2S$ $[M+H]^+$ 287.0404. Found: 287.0402.

#### 3.1.3.2. 2-(3-Chlorophenylthio)-3-methylquinoxaline (2b)

Yield 94% (755 mg). White solid. Mp 97 °C. **$^1$H NMR (250 MHz, $CDCl_3$)** $\delta$ 7.98 – 7.94 (m, 1H), 7.74 – 7.69 (m, 1H), 7.65 – 7.55 (m, 3H), 7.52 – 7.33 (m, 3H), 2.78 (s, 3H). **$^{13}$C NMR (63 MHz, $CDCl_3$)** $\delta$ 155.0, 151.4, 141.4, 139.8, 134.9, 134.8, 133.3, 130.5, 130.3, 130.2, 129.5, 129.3, 128.8, 128.2, 22.4. **LC-MS** (ESI+) $t_R$ 6.83 min; m/z $[M+H]^+$ 286.36/289.04. MW: 286.78 g.mol$^{-1}$.**HRMS (ESI)**: m/z calcd. for $C_{15}H_{11}ClN_2S$ $[M+H]^+$ 287.0404. Found: 287.0402.

#### 3.1.3.3. 2-(2,3-Dichlorophenylthio)-3-methylquinoxaline (2c)

Yield 100% (899 mg). Brown solid. Mp 142 °C. **$^1$H NMR (250 MHz, $CDCl_3$)** $\delta$ 7.92 – 7.88 (m, 1H), 7.65 – 7.49 (m, 5H), 7.23 – 7.20 (m, 1H), 2.76 (s, 3H).**$^{13}$C NMR (63 MHz, $CDCl_3$)** $\delta$ 154.0, 151.5, 141.4, 140.0, 137.7, 135.6, 134.1, 131.7, 130.9, 129.2, 128.9, 128.3, 128.2, 127.6, 22.5. **LC-MS** (ESI+) $t_R$ 4.69 min;

m/z [M+H] $^{+}$ 319.75/322.54. MW: 321.22 g.mol$^{-1}$. **HRMS (ESI) :** m/z [M+H]$^{+}$ calcd for $C_{15}H_{10}Cl_2N_2S$:, 321.0015 Found: 321.0013.

#### 3.1.3.4. 2-(2,4-Dichlorophenylthio)-3-methylquinoxaline (2d)

Yield 80% (719 mg). Brown solid. Mp 116 °C. $^{1}$H NMR (400 MHz, $CDCl_3$) δ 7.97 – 7.91 (m, 1H), 7.70 – 7.66 (m, 1H), 7.65 – 7.54 (m, 4H), 7.34 (dd, *J* = 8.3, 2.2 Hz, 1H), 2.80 (s, 3H). $^{13}$C NMR (101 MHz, $CDCl_3$) δ 154.0, 151.4, 141.5, 140.5, 140.0, 138.4, 136.5, 130.3, 129.2, 128.8, 128.4, 128.2, 127.8, 127.0, 22.5. **LC-MS** (ESI+) $t_R$ 0.74 min; m/z [M+H]$^{+}$ 320.94/322.85/325.10. MW: 321.22 g.mol$^{-1}$**. HRMS (ESI):** m/z [M+H]$^{+}$ calcd for $C_{15}H_{10}Cl_2N_2S$: 321.0015, Found: 321.0013.

#### 3.1.3.5. 2-(2-Fluorophenylthio)-3-methylquinoxaline (2e)

Yield 78% (590 mg). Brown solid. Mp 159 °C. **$^{1}$H NMR (250 MHz, $CDCl_3$)** *δ* 8.03 – 7.85 (m, 1H), 7.69 – 7.47 (m, 4H), 7.28 – 7.20 (m, *J* = 19.4 Hz, 3H), 2.82 (s, 3H). **$^{13}$C NMR (63 MHz, $CDCl_3$)** *δ* 163.3 (d, *J* = 249.6 Hz), 154.3, 151.3, 141.5, 139.9, 137.3, 132.01 (d, *J* = 8.2 Hz), 129.1, 128.6, 128.3, 128.2, 124.8 (d, *J* = 3.8 Hz), 116.3 (d, *J* = 22.9 Hz), 115.8, 22.5. **LC-MS** (ESI+) $t_R$ 3.90 min; m/z [M+H]$^{+}$ 271.10. MW: 270.32 g.mol$^{-1}$. **HRMS (ESI) :** m/z [M+H]$^{+}$ calcd for $C_{15}H_{11}FN_2S$: 271.0700, Found: 271.0699.

#### 3.1.3.6. 2-(3-Fluorophenylthio)-3-methylquinoxaline (2f)

Yield 95% (719 mg). Brown solid. Mp 92 °C. **$^{1}$H NMR (250 MHz, $CDCl_3$)** *δ* 7.92 – 7.89 (m, 1H), 7.74 – 7.70 (m, 1H), 7.63 – 7.53 (m, 2H), 7.48 – 7.36 (m, 3H), 7.20 – 7.12 (m, 1H), 2.77 (s, 3H). **$^{13}$C NMR (63 MHz, $CDCl_3$)** *δ* 162.8 (d, *J* = 248.5 Hz), 155.0, 151.5, 141.4, 139.9, 130.8, 130.7 (d, *J* = 3.2 Hz), 130.4 (d, *J* = 8.3 Hz), 129.3, 128.8, 128.3, 128.2, 122.1 (d, *J* = 22.6 Hz), 116.4 (d, *J* = 21.1 Hz), 22.5. **LC-MS** (ESI+) $t_R$ 4.24 min; m/z [M+H] $^{+}$ 271.26. MW: 270.32 g.mol$^{-1}$. **HRMS (ESI):** m/z [M+H]$^{+}$ calcd for $C_{15}H_{11}FN_2S$: 271.0700, Found: 271.0698.

#### 3.1.3.7. 2-(4-Fluorophenylthio)-3-methylquinoxaline (2g)

Yield 98% (742 mg). orange solid. Mp 115 °C. **$^{1}$H NMR (250 MHz, $CDCl_3$)** *δ* 7.93 (dd, *J* = 6.5, 3.2 Hz, 1H), 7.69 – 7.52 (m, 5H), 7.17 (t, *J* = 8.7 Hz, 2H), 2.77 (s, 3H). **$^{13}$C NMR (63 MHz, $CDCl_3$)** *δ* 163.6 (d, *J* = 249.5 Hz), 155.8, 151.3, 141.4, 139.8, 137.7 (d, *J* = 8.5 Hz), 129.2, 128.6, 128.2, 128.1, 123.7 (d, *J* = 3.4 Hz), 116.5 (d, *J* = 22.1 Hz), 22.4. **LC-MS** (ESI+) $t_R$ 4.20 min; m/z [M+H] $^{+}$ 271.24. MW: 270.32 g.mol$^{-1}$. **HRMS (ESI):** m/z [M+H]$^{+}$ calcd for $C_{15}H_{11}FN_2S$: 271.0700, Found: 271.0699.

#### 3.1.3.8. 2-(2-Methoxyphenylthio)-3-methylquinoxaline (2h)

Yield 72% (569 mg). Brown solid. Mp 138 °C. **$^{1}$H NMR (400 MHz, $CDCl_3$)** *δ* 7.93 (dd, *J* = 8.1, 1.5 Hz, 1H), 7.67 – 7.62 (m, 1H), 7.58 (dd, *J* = 7.5, 1.6 Hz, 1H), 7.56 – 7.50 (m, 2H), 7.51 – 7.43 (m, 1H), 7.08 – 6.99 (m, 2H), 3.76 (s, 3H), 2.81 (s, 3H). **$^{13}$C NMR (101 MHz, $CDCl_3$)** *δ* 160.3, 155.3, 151.9, 141.6, 139.9, 137.0, 131.4, 128.8, 128.3, 128.1, 128.1, 121.3, 116.9, 111.8, 56.2, 22.6. **LC-MS** (ESI+) $t_R$ 3.61 min; m/z [M+H]$^{+}$ 283.19. MW: 282.36 g.mol$^{-1}$. **HRMS (ESI):** m/z [M+H]$^{+}$ calcd for $C_{16}H_{14}N_2OS$: 283.0900, Found: 283.0899.

#### 3.1.3.9. 2-(3-Methoxyphenylthio)-3-methylquinoxaline (2i)

Yield 100% (791 mg). orange solid. Mp 103 °C. **$^{1}$H NMR (400 MHz, $CDCl_3$)** *δ* 7.95 – 7.91 (m, 1H), 7.74 – 7.72 (m, 1H), 7.61 – 7.53 (m, 2H), 7.38 – 7.34 (m, 1H), 7.21 – 7.19 (m, 2H), 7.00 (m, 1H), 3.83 (s, 3H), 2.77 (s, 3H). **$^{13}$C NMR (101 MHz, $CDCl_3$)** *δ* 160.0, 155.7, 151.8, 141.5, 139.9, 130.0, 129.8, 129.1, 128.6, 128.2, 128.2, 127.2, 120.0, 115.5, 55.6, 22.6. **LC-MS** (ESI+) $t_R$ 4.12 min; m/z [M+H]$^{+}$ 283.28. MW: 282,36 g.mol$^{-1}$. **HRMS (ESI) :** m/z [M+H]$^{+}$ calcd for $C_{16}H_{14}N_2OS$: 283.0900, Found: 283.0898.

#### 3.1.3.10. 2-(4-Methoxyphenylthio)-3-methylquinoxaline (2j)

Yield 39% (308 mg). White solid. Mp 113 °C. **$^1$H NMR (250 MHz, $CDCl_3$)** $\delta$ 7.96 – 7.88 (m, 1H), 7.71 – 7.65 (m, 1H), 7.60 – 7.50 (m, 4H), 7.03 – 6.97 (m, 2H), 3.88 (s, 3H), 2.77 (s, 3H). **$^{13}$C NMR (63 MHz, $CDCl_3$)** $\delta$ 160.7, 156.7, 151.5, 141.5, 139.8, 137.2 (2C), 129.0, 128.3, 128.2, 128.1, 119.0, 114.9 (2C), 55.5, 22.5. **LC-MS** (ESI+) $t_R$ 4.12 min; m/z $[M+H]^+$283.20. MW: 282.36 g.mol$^{-1}$. **HRMS (ESI):** m/z $[M+H]^+$ calcd for $C_{16}H_{14}N_2OS$: 283.0900, Found: 283.0901.

#### 3.1.3.11. 2-Methyl-3-(phenylthio)quinoxaline (2k)

Yield **87%** (615 mg). Red solid. Mp 134 °C. **$^1$H NMR (400 MHz, $CDCl_3$)** δ 7.95 – 7.89 (m, 1H), 7.71 – 7.66 (m, 1H), 7.65 – 7.60 (m, 2H), 7.60 – 7.51 (m, 2H), 7.49 – 7.04 (m, 3H), 2.78 (s, 3H) . **$^{13}$C NMR (101 MHz, $CDCl_3$** δ 155.8, 151.7, 141.5, 140.1, 135.3(2C), 129.3(2C), 129.2, 129.0, 128.9, 128.4, 128.3, 128.2, 22.6. **LC-MS** (ESI+) $t_R$ 4.05 min; m/z $[M+H]^+$ 253.28. MW: 252.33 g.mol$^{-1}$. **Chemical Formula**: $C_{15}H_{12}N_2S$. **HRMS (ESI):** m/z $[M+H]^+$ calcd for $C_{15}H_{12}N_2S$: 253.0794, Found: 253.0789.

#### 3.1.3.12. 2-(4-Bromophenylthio)-3-methylquinoxaline (2l)

Yield 99% (918 mg). White solid. Mp 121 °C. **$^1$H NMR (250 MHz, $CDCl_3$)** $\delta$ 7.95 – 7.91 (m, 1H), 7.72 – 7.68 (m, 1H), 7.61 – 7.54 (m, 4H), 7.49 – 7.46 (m, 2H), 2.77 (s, 3H). **$^{13}$C NMR (63 MHz, $CDCl_3$)** $\delta$ 155.1, 151.5, 141.4, 140.1, 136.9 (2C), 132.4 (2C), 129.2, 128.6, 128.3, 128.1, 127.8, 123.8, 22.5. **LC-MS** (ESI+) $t_R$ 4.81 min; m/z $[M+H]^+$ 331.00/333.08/334.19. MW: 331.23 g.mol$^{-1}$. **HRMS (ESI):** m/z $[M+H]^+$ calcd for $C_{15}H_{11}BrN_2S$: 332.9879, Found: 332.9879.

#### 3.1.3.13. 2-Methyl-3-(4-trifluoromethylphenylthio)quinoxaline (2m)

Yield 87% (780 mg). Beige solid. Mp 99 °C. **$^1$H NMR (250 MHz, $CDCl_3$)** $\delta$ 7.98 – 7.94 (m, 1H), 7.77 – 7.69 (m, 5H), 7.66 – 7.54 (m, 2H), 2.79 (s, 3H). **$^{13}$C NMR (63 MHz, $CDCl_3$)** $\delta$ 154.5, 151.6, 141.3, 140.1, 135.1, 133.8 (q, $J$ = 1.5), 131.1 (q, $J$ = 32.7 Hz), 130.8, 129.3, 128.9, 128.4, 128.1, 126.2, 126.0 (q, $J$ = 3.7 Hz), 124.2 (q, $J$ = 272.36 Hz), 22.5. **LC-MS** (ESI+) $t_R$ 4.70 min; m/z $[M+H]^+$ 319.78. MW: 320.33 g.mol$^{-1}$. **HRMS (ESI):** m/z $[M+H]^+$ calcd for $C_{16}H_{11}F_3N_2S$: 321.0668, Found: 321.0663.

#### 3.1.3.14. 2-Methyl-3-(4-trifluoromethoxyphenylthiol)quinoxaline (2n)

Yield 89% (838 mg). Yellow solid. Mp 81 °C. **$^1$H NMR (250 MHz, $CDCl_3$)** δ 7.94 (m, 1H), 7.71 – 7.62 (m, 3H), 7.62 – 7.54 (m, 2H), 7.31 (d, $J$ = 8.0 Hz, 2H), 2.78 (s, 3H). **$^{13}$C NMR (63 MHz, $CDCl_3$)** δ 155.2, 151.4, 150.0 (q, $J$ = 1.8 Hz), 141.4, 140.1, 137.0 (2C), 129.2, 128.7, 128.4, 128.1, 127.2, 121.5 (2C), 120.6 (q, $J$ = 257.9 Hz), 22.5. **LC-MS** (ESI+) $t_R$ 4.97 min; m/z $[M+H]^+$ no ionization. MW: 336.33 g.mol$^{-1}$. **HRMS (ESI):** m/z $[M+H]^+$ calcd for $C_{16}H_{11}F_3N_2OS$: 337.0617, Found: 337.0615.

#### 3.1.3.15. 2-Methyl-3-(4-nitrophenylthio)quinoxaline (2o)

Yield 86% (716 mg). Brown solid. Mp 163 °C. **$^1$H NMR (250 MHz, $CDCl_3$)** δ 8.35 – 8.25 (m, 2H), 8.00 – 7.93 (m, 1H), 7.84 – 7.76 (m, 2H), 7.75 – 7.70 (m, 1H), 7.68 – 7.59 (m, 2H), 2.80 (s, 3H). **$^{13}$C NMR (101 MHz, $CDCl_3$)** δ 153.5, 151.7, 148.0, 141.2, 140.4, 138.2, 134.9 (2C), 129.6, 129.3, 128.5, 128.1, 124.0 (2C), 22.5. **LC-MS** (ESI+) $t_R$ 4.26 min; m/z $[M+H]^+$ 298.16. MW: 297.33 g.mol$^{-1}$**. HRMS (ESI):** m/z $[M+H]^+$ calcd for $C_{15}H_{11}N_3O_2S$: 298.0645, Found: 298.0645.

#### 3.1.3.16. 2-Methyl-3-(4-tolylthio)quinoxaline (2p)

Yield 74% (552 mg). Brown solid. Mp 92 °C. **$^1$H NMR (400 MHz, $CDCl_3$)** δ 7.96 – 7.89 (m, 1H), 7.73 – 7.67 (m, 1H), 7.59 – 7.52 (m, 2H), 7.52 – 7.47 (m, 2H), 7.30 – 7.26 (m, 2H), 2.77 (s, 3H), 2.43 (s, 3H). **$^{13}$C NMR (101 MHz, $CDCl_3$)** δ 156.2, 151.7, 141.5, 139.9, 139.5, 135.3 (2C), 130.1 (2C), 128.9, 128.3, 128.3, 128.2, 125.1, 22.5, 21.5. **LC-MS** (ESI+) $t_R$ 0.71 min; m/z $[M+H]^+$ 266.66. MW: 266.36 g.mol$^{-1}$**.** **HRMS (ESI):** m/z $[M+H]^+$ calcd for $C_{16}H_{14}N_2S$: 267.0950, Found: 267.0948.

### 3.1.4. General procedure for the preparation of 2-thiophenoxy-3-trichloromethylquinoxaline derivatives

To a solution of 2-methyl-3-substituted quinoxaline (**2a-2p**) (624 mg, 2.8 mmol) and $PCl_5$ (2.88 g, 16.8 mmol, 1.0 equiv), $POCl_3$ was added to make a slurry (ca.5 mL). The mixture was then heated in a multimode microwave oven at 100 °C, 800 W for 20 – 30 min. After completion of the reaction, the mixture was poured into ice and was then neutralized with $Na_2CO_3$. The resulting solution was extracted with $CH_2Cl_2$ and dried with $Na_2SO_4$. After filtration and evaporation, the resulting solid was purified by silica gel column chromatography (eluent: Petroleum Ether/$CH_2Cl_2$, 9:1) to afford the desired compound.

#### 3.1.4.1. 2-(2-Chlorophenylthio)-3-trichloromethylquinoxaline (3a)

Yield 62% (675 mg). White solid. Mp 127 °C (isopropanol). **$^1$H NMR (250 MHz, $CDCl_3$)** $\delta$ 8.14 – 8.07 (m, 1H), 7.75 – 7.62 (m, 4H), 7.59 – 7.55 (m, 1H), 7.44 (dt, *J* = 7.6, 1.9 Hz, 1H), 7.33 (dt, *J* = 7.4, 1.6 Hz, 1H). **$^{13}$C NMR (63 MHz, $CDCl_3$)** δ = 152.1, 147.4, 141.9, 139.9, 138.1, 136.8, 132.0, 131.2, 130.4, 129.8, 129.7, 129.5, 127.9, 127.5, 96.5**. LC-MS** (ESI+) $t_R$ 5.4 min, m/z [M+H] $^+$no ionization, purity 99%. MW: 390.11 g.mol$^{-1}$. **HRMS m/z** [M+H]$^+$ calcd for $C_{15}H_8Cl_4N_2S$: 388.9235, Found: 388.9240.

#### 3.1.4.2. 2-(3-Chlorophenylthio)-3-trichloromethylquinoxaline (3b)

Yield 74% (437 mg). White solid. Mp 81 °C (isopropanol). **$^1$H NMR (250 MHz, $CDCl_3$)** $\delta$ 8.13 – 8.07 (m, 1H), 7.73 – 7.65 (m, 4H), 7.52 (dt, *J* = 7.2, 1.6 Hz, 1H), 7.47 – 7.36 (m, 2H). **$^{13}$C NMR (63 MHz, $CDCl_3$)** δ = 152.4, 147.3, 141.8, 136.8, 135.4, 134.7, 133.8, 132.1, 131.6, 130.2, 129.9, 129.7, 129.6, 127.8, 96.5. **LC-MS** (ESI+) $t_R$ 5.7 min, m/z [M+H] $^+$378.96/380.90/386.38, purity 99%. MW: 390.11 g.mol$^{-1}$. **HRMS m/z** [M+H]$^+$ calcd for $C_{15}H_8Cl_4N_2S$: 388.9235, Found: 388.9235.

#### 3.1.4.3. 2-(2,3-Dichlorophenylthio)-3-(trichloromethyl)quinoxaline (3c)

Yield 61% (725 mg). Beige solid. Mp 91 °C (isopropanol). **$^1$H NMR (400 MHz, $CDCl_3$)** $\delta$ 8.13 – 8.09 (m, 1H), 7.74 – 7.62 (m, 4H), 7.60 (dd, *J* = 8.1, 1.5 Hz, 1H), 7.30 (t, *J* = 7.9 Hz, 1H). **$^{13}$C NMR (101 MHz, $CDCl_3$)** δ = 151.5, 147.4, 141.9, 138.1, 136.8, 136.2, 134.2, 132.2, 132.0, 131.9, 130.0, 129.8, 127.9, 127.6, 96.4 . **LC-MS** (ESI+) $t_R$ 5.7 min, m/z [M+H]$^+$ no ionization, purity 99%. MW: 424.56 g.mol$^{-1}$ . HRMS m/z [M+H]$^+$ calcd for $C_{15}H_7N_2SCl_5$: 424.8816, Found: 424.8808.

#### 3.1.4.4. 2-(2,4-Dichlorophenylthio)-3-trichloromethylquinoxaline (3d)

Yield 46% (547 mg). Yellow solid. Mp 97 °C (isopropanol). $^1$H NMR (400 MHz, DMSO) $\delta$ 8.13 – 8.04 (m, 1H), 7.77 – 7.63 (m, 4H), 7.58 (d, *J* = 2.2 Hz, 1H), 7.40 – 7.32 (m, 1H). $^{13}$C NMR (101 MHz, DMSO) $\delta$ 151.8, 147.7, 142.1, 141.2, 139.1, 137.1, 137.0, 132.5, 130.6, 130.3, 130.1, 128.4, 128.1 (2C), 96.7. **LC-MS** (ESI+) $t_R$ 6.07 min, m/z [M+H] $^+$no ionization, purity 98%. MW: 424.56 g.mol$^{-1}$. **HRMS m/z** [M+H]$^+$ calcd $C_{15}H_7N_2SCl_5$: 424.8816, Found: 424.8808.

#### 3.1.4.5. 2-(2-Fluorophenylthio)-3-trichloromethylquinoxaline (3e)

Yield 56% (555 mg). Beige solid. Mp 104 °C (isopropanol). **$^1$H NMR (400 MHz, $CDCl_3$)** $\delta$ 8.11 – 8.06 (m, 1H), 7.70 – 7.61 (m, 4H), 7.53 – 7.47 (m, 1H), 7.26 – 7.19 (m, 2H). **$^{13}$C NMR (101 MHz, $CDCl_3$)** δ = 163.3 (d, *J* = 250.0 Hz), 151.7, 147.3, 141.9, 137.4, 136.8, 132.2 (d, *J* = 8.2 Hz), 132.0, 129.8, 129.7, 127.8, 124.8 (d, *J* = 3.8 Hz), 117.3 (d, *J* = 18.8 Hz), 116.2 (d, *J* = 22.8 Hz), 96.5 . **LC-MS** (ESI+) $t_R$ 5.2 min,

m/z $[M+H]^+$ no ionization, purity 99%. MW: 353.66 g.mol$^{-1}$. **HRMS m/z** $[M+H]^+$ calcd for $C_{15}H_8N_2FSCl_3$: 374.9502, Found: 374.9492.

#### 3.1.4.6. 2-(3-Fluorophenylthio)-3-trichloromethylquinoxaline (3f)

Yield 63% (659 mg). Beige solid. Mp 57 °C (isopropanol). **$^1$H NMR (400 MHz, $CDCl_3$)** $\delta$ 8.12 – 8.06 (m, 1H), 7.73 – 7.64 (m, 3H), 7.45 – 7.40 (m, 3H), 7.22 – 7.15 (m, 1H). **$^{13}$C NMR (101 MHz, $CDCl_3$)** δ = 162.6 (d, *J* = 248.9 Hz), 152.3, 147.2, 141.6, 136.6, 131.9, 131.7 (d, *J* = 8.0 Hz), 131.2 (d, *J* = 3.0 Hz), 130.3 (d, *J* = 8.1 Hz), 129.8, 129.6, 127.65, 122.5 (d, *J* = 22.3 Hz), 116.5 (d, *J* = 21.0 Hz), 96.5 . **LC-MS** (ESI+) $t_R$ 5.4 min, m/z $[M+H]^+$ no ionization, purity 99%. MW: 373.66 g.mol$^{-1}$. **HRMS m/z** $[M+H]^+$ calcd for $C_{15}H_8N_2SFCl_3$: 374.9502, Found: 374.9495.

#### 3.1.4.7. 2-(4-Fluorophenylthio)-3-trichloromethylquinoxaline (3g)

Yield 51% (534 mg). Yellow solid. Mp 76 °C (isopropanol). **$^1$H NMR (400 MHz, $CDCl_3$)** $\delta$ 8.09 – 8.08 (m, 1H), 7.69 – 7.61 (m, 5H), 7.18 (t, *J* = 8.6 Hz, 2H). **$^{13}$C NMR (101 MHz, $CDCl_3$)** δ = 163.6 (d, *J* = 250.0 Hz), 153.1, 147.1, 141.7, 138.1 (d, *J* = 8.6 Hz) (2C), 136.6, 131.9, 129.6, 127.6, 124.8 (d, *J* = 3.4 Hz), 116.4 (d, *J* = 22.0 Hz) (2C), 96.6. **LC-MS** (ESI+) $t_R$ 5.4 min, m/z $[M+H]^+$ no ionization, purity 99%. MW: 373.66 g.mol$^{-1}$ . **HRMS m/z** $[M+H]^+$ calcd for $C_{15}H_8N_2SFCl_3$: 374.9502, Found: 374.9494.

#### 3.1.4.8. 2-(2-Methoxyphenylthio)-3-trichloromethylquinoxaline (3h)

Yield 64% (691 mg). Yellow solid. Mp 96 °C (isopropanol). **$^1$H NMR (400 MHz, $CDCl_3$)** $\delta$ 8.10 – 8.06 (m, 1H), 7.65 – 7.61 (m, 4H), 7.48 (td, *J* = 8.2, 1.6 Hz, 1H), 7.05 (td, *J* = 7.5, 0.9 Hz, 1H), 7.00 (d, *J* = 8.2 Hz, 1H), 3.69 (s, 3H). **$^{13}$C NMR (101 MHz, $CDCl_3$)** δ = 160.1, 152.9, 147.6, 142.0, 137.1, 136.6, 131.8, 131.6, 129.7, 129.4, 127.7, 121.2, 118.4, 111.6, 96.7, 56.1. **LC-MS** (ESI+) $t_R$ 5.1 min, m/z $[M+H]^+$ no ionization, purity 99%. MW: 385.70 g.mol$^{-1}$ . **HRMS** m/z $[M+H]^+$ calcd for $C_{16}H_{11}N_2OSCl_3$: 386.9702, Found: 386.9698.

#### 3.1.4.9. 2-(2-Chloro-5-methoxyphenylthio)-3-trichloromethylquinoxaline (3i)

Yield 15% (176 mg). Yellow solid. Mp 144 °C (isopropanol). **$^1$H NMR (250 MHz, $CDCl_3$)** $\delta$ 8.16 – 8.06 (m, 1H), 7.77 – 7.63 (m, 3H), 7.51 – 7.40 (m, 1H), 7.27 (d, *J* = 3.0 Hz, 1H), 6.98 (dd, *J* = 8.8, 3.0 Hz, 1H), 3.84 (s, 3H).**$^{13}$C NMR (63 MHz, $CDCl_3$)** δ = 158.51, 151.94, 147.40, 141.97, 136.80, 132.06, 131.06, 130.74, 130.07, 129.84, 129.77, 127.93, 122.66, 117.23, 96.54, 55.89. **LC-MS** (ESI+) $t_R$ 7.4 min, m/z $[M+H]^+$ no ionization, purity = 99%. MW: 420.14 g.mol$^{-1}$. **HRMS m/z** $[M+H]^+$ calcd for $C_{16}H_{10}Cl_4N_2OS$: 420.9312, Found: 420.9312.

#### 3.1.4.10. 2-(4-Methoxyphenylthio)-3-trichloromethylquinoxaline (3j)

Yield 59% (637 mg). Yellow solid. Mp 149 °C (isopropanol). **$^1$H NMR (250 MHz, $CDCl_3$)** $\delta$ 8.10 – 8.05 (m, 1H), 7.72 – 7.63 (m, 3H), 7.55 (dt, *J* = 2.5; 9.0 Hz, 2H), 6.99 (dt, *J* = 2.6; 8.8 Hz, 2H), 3.89 (s, 3H). **$^{13}$C NMR (63 MHz, $CDCl_3$)** δ = 160.8, 154.1, 147.2, 141.9, 137.7 (2 C), 136.7, 131.9, 129.7, 129.5, 127.8, 120.2, 114.9 (2 C), 96.7, 55.5. **LC-MS** (ESI+) $t_R$ 5.4 min, m/z $[M+H]^+$ no ionization, purity = 99%. MW: 385.70 g.mol$^{-1}$. **HRMS m/z** $[M+H]^+$ calcd for $C_{16}H_{11}N_2OSCl_3$: 386.9702, Found: 386.9699.

#### 3.1.4.11. 2-(Phenylthio)-3-trichloromethylquinoxaline (3k)

Yield 71% (707 mg). Beige solid. Mp 66 °C (isopropanol). **$^1$H NMR (400 MHz, $CDCl_3$)** $\delta$ 8.12 – 8.07 (m, 1H), 7.72 – 7.67 (m, 3H), 7.66 – 7.62 (m, 2H), 7.48 – 7.46 (m, 3H). **$^{13}$C NMR (101 MHz, $CDCl_3$)** δ =

153.4, 147.4, 141.9, 136.8, 135.8 (3 C), 131.9, 129.9, 129.7, 129.4, 129.3 (2 C), 127.8, 96.7**. LC-MS** (ESI+) $t_R$ 5.3 min, m/z $[M+H]^+$ no ionization, purity 98%. MW: 355.67 g.mol$^{-1}$. **HRMS m/z** $[M+H]^+$ calcd for $C_{15}H_9N_2SCl_3$: 356.9596, Found: 356.9594.

#### 3.1.4.12. 2-(4-Bromophenylthio)-3-trichloromethylquinoxaline (3l)

Yield 44% (535 mg). Beige solid. Mp 96 °C (isopropanol). **$^1$H NMR (250 MHz, $CDCl_3$)** $\delta$ 8.14 – 8.06 (m, 1H), 7.74 – 7.66 (m, 3H), 7.62 – 7.56 (m, 2H), 7.51 – 7.46 (m, 2H). **$^{13}$C NMR (101 MHz, $CDCl_3$)** δ = 152.6, 147.3, 141.8, 137.4 (2 C), 136.8, 132.4 (2 C), 132.1, 129.9, 129.7, 128.9, 127.8, 124.1, 96.5. **LC-MS** (ESI+) $t_R$ 5.8 min, m/z $[M+H]^+$ no ionization, purity 99%. MW: 434.57 g.mol$^{-1}$ . **HRMS m/z** $[M+H]^+$ calcd for $C_{15}H_8N_2SCl_3Br$: 434.8705, Found: 434.8701.

#### 3.1.4.13. 2-Trichloromethyl-3-(4-trifluoromethylphenylthio)quinoxaline (3m)

Yield 80% (949 mg). Yellow solid. Mp 102 °C (isopropanol).**$^1$H NMR (250 MHz, $CDCl_3$)** $\delta$ 8.23 – 7.96 (m, 1H), 7.86 – 7.54 (m, 7H). **$^{13}$C NMR (63 MHz, $CDCl_3$)** δ = 152.0, 147.5, 141.8, 136.9, 135.6, 134.9 (d, *J* = 1.4 Hz), 132.3, 131.3 (q, *J* = 32.7 Hz), 130.2, 129.8, 127.8, 126.0 (q, *J* = 3.7 Hz), 124.1 (q, *J* = 272.4 Hz), 96.5. **LC-MS** (ESI+) $t_R$ 5.38 min, m/z $[M+H]^+$ no ionization. MW: 423.67 g.mol$^{-1}$, purity 99%. **HRMS m/z** $[M+H]^+$ calcd for $C_{16}H_8Cl_3F_3N_2S$: 424.9470, Found: 424.9468.

#### 3.1.4.14. 2-Trichloromethyl-3-(4-trifluoromethoxyphenylthio)quinoxaline (3n)

Yield 68% (837 mg). Yellow oil. **$^1$H NMR (250 MHz, $CDCl_3$)** $\delta$ 8.16 – 8.06 (m, 1H), 7.76 – 7.62 (m, 5H), 7.36 – 7.28 (m, 2H). **$^{13}$C NMR (63 MHz, $CDCl_3$)** δ = 152.7, 150.2 (q, *J* = 1.7 Hz), 147.4, 141.8, 137.5 (2C), 136.8, 132.2, 129.9, 129.8, 128.3, 127.8, 121.5 (2C), 120.6(q, *J* = 258.0 Hz), 96.5. **LC-MS** (ESI+) $t_R$ 6.1 min, m/z $[M+H]^+$ no ionization. MW: 439.67 g.mol$^{-1}$, purity 99%. **HRMS m/z** $[M+H]^+$ calcd for $C_{16}H_8Cl_3F_3N_2OS$: 438.9448, Found: 438.9447.

#### 3.1.4.15. 2-(4-Nitrophenylthio)-3-trichloromethylquinoxaline (3o)

Yield 64% (718 mg). White solid. Mp 161 °C (isopropanol). **$^1$H NMR (250 MHz, $CDCl_3$)** $\delta$ 8.34 – 8.23 (m, 2H), 8.20 – 8.10 (m, 1H), 7.88 – 7.67 (m, 5H). **$^{13}$C NMR (63 MHz, $CDCl_3$)** δ = 151.1, 148.1, 147.7, 141.8, 139.2, 137.1, 135.4 (2C), 132.6, 130.6, 129.9, 127.7, 124.1 (2C), 96.3. **LC-MS** (ESI+) $t_R$ 4.9 min, m/z $[M+H]^+$ no ionization. MW: 400.67 g.mol$^{-1}$, purity 99%. **HRMS m/z** $[M+H]^+$ calcd for $C_{15}H_8Cl_3N_3O_2S$: 401.9447, Found: 401.9447.

#### 3.1.4.16. 2-(4-Tolylthio)-3-trichloromethylquinoxaline (3p)

Yield 40% (414 mg). Yellow solid. Mp 99 °C (isopropanol). **$^1$H NMR (400 MHz, $CDCl_3$)** $\delta$ 8.13 – 8.04 (m, 1H), 7.76 – 7.64 (m, 3H), 7.56 – 7.46 (m, 2H), 7.30 – 7.23 (m, 2H), 2.44 (s, 3H). **$^{13}$C NMR (101 MHz, $CDCl_3$)** δ = 153.7, 147.4, 142.0, 139.7, 136.7, 135.8 (2C), 131.9, 130.1 (2C), 129.7, 129.6, 127.8, 126.2, 96.7, 21.6. **LC-MS** (ESI+) $t_R$ 5.67 min, m/z $[M+H]^+$ 368.18/371.01/373.05. MW: 369.70 g.mol$^{-1}$, purity 99%. **HRMS m/z** $[M+H]^+$ calcd for $C_{16}H_{11}Cl_3N_2S$: 370.9753, Found: 370.9752.

### 3.1.5. General procedure for compounds 3q-3s

#### 3.1.5.1. Preparation of 2-chloro-3-(trifluoromethyl)quinoxaline (3q)

**Step 1**: To a solution of *o*-phenylenediamine (2g, 18.5 mmol, 1.0 equiv) in $H_2O$ was added ethyl trifluoropyruvate (3g 146, 18.5 mmol, 1.0 equiv) dissolved in $H_2O$ (30 mL). The reaction mixture was heated at 50 °C for 15 min. After cooling, the precipitate was filtered off and washed with $H_2O$. 3-

(Trifluoromethyl)quinoxalin-2(*1H*)-one was recrystallized from ethanol, precipitating as a white solid and engaged directly in step 2. Yield 93%.

**Step 2**: 3-(Trifluoromethyl)quinoxalin-2-ol (3.5 g, 16.8 mmol, 1.0 equiv) was heated to reflux in phosphorus oxychloride (30 mL) for 2 h. After the starting material was consumed, the reaction mixture was cooled to r.t. and then quenched with ice at 0 °C. The precipitate was purified by flash chromatography, to afford 2-chloro-3-(trifluoromethyl)quinoxaline (3q) as a white solid, yield 96%. Mp 140 °C. **$^1$H NMR (400 MHz, $CDCl_3$)** δ 8.25 – 8.20 (m, 1H), 8.15 – 8.09 (m, 1H), 7.99 – 7.86 (m, 2H). NMR was consistent with description [44].

#### 3.1.5.2. Preparation of compounds (3r, 3s)

To a solution of 2-chloroquinoxaline or 2-chloro-3-(trifluoromethyl)quinoxaline (300 mg, 1.3 mmol, 1.0 equiv.) and thiophenol reagent (143 mg, 1.3 mmol, 1.0 equiv.) in anhydrous DMF (5 mL), $Cs_2CO_3$ (1.0 equiv.) was added under inert atmosphere. The mixture was stirred at 70 °C overnight. After completion of the reaction, water was added, leading to a precipitate which was separated by filtration. The resulting precipitate was then thoroughly washed with water. The resulting solid was purified by silica gel column chromatography (eluent: Cyclohexane/$CH_2Cl_2$, 4:6) to afford the desired compound.

##### 3.1.5.2.1. 2-(Phenylthio)quinoxaline (3r)

Yield 90% (279 mg). orange solid. Mp 88 °C (isopropanol). **$^1$H NMR (400 MHz, $CDCl_3$)** *δ* 8.44 (s, 1H), 7.99 (dd, *J* = 8.2, 1.4 Hz, 1H), 7.90 (dd, *J* = 8.3, 1.3 Hz, 1H), 7.73 – 7.60 (m, 4H), 7.50 – 7.44 (m, 3H). **$^{13}$C NMR (101 MHz, $CDCl_3$)** δ = 157.3, 143.6, 142.3, 140.0, 135.1 (2C), 130.6, 129.9 (2C), 129.8, 129.3, 129.1, 128.9, 128.4. **LC-MS** (ESI+) $t_R$ 3.4 min, m/z $[M+H]^+$ 239.16. MW: 238.31 g.mol$^{-1}$, purity 99%. **HRMS m/z** $[M+H]^+$ calcd for $C_{14}H_{10}N_2S$: 239.0637, Found: 239.0638.

##### 3.1.5.2.2. 2-(Phenylthio)-3-(trifluoromethyl)quinoxaline (3s)

Yield 89% (354 mg). white solid. Mp 93 °C (isopropanol). **$^1$H NMR (400 MHz, $CDCl_3$)** *δ* 8.14 – 8.07 (m, 1H), 7.75 – 7.67 (m, 3H), 7.66 – 7.61 (m, 2H), 7.51 – 7.45 (m, 3H). **$^{13}$C NMR (101 MHz, $CDCl_3$)** δ = 153.5, 143.0, 139.8 (q, *J* = 35.8 Hz), 137.9, 136.0 (2C), 132.5, 129.8, 129.8, 129.4 (2C), 129.2, 128.3, 127.9 (d, *J* = 1.9 Hz), 121.2 (q, *J* = 276.0 Hz). **LC-MS** (ESI+) $t_R$ 6.8 min, m/z $[M+H]^+$ 307.07. MW: 306.31 g.mol$^{-1}$, purity 99%. **HRMS m/z** $[M+H]^+$ calcd for $C_{15}H_9F_3N_2S$: 307.0511, Found: 307.0511.

### 3.2. Biology

#### 3.2.1. *In Vitro* Cytotoxicity Evaluation HepG2

HepG2 cell line was maintained at 37 °C, 5% $CO_2$, at 90% humidity in MEM supplemented with 10% fetal bovine serum, 1% L-glutamine (200 mM) and penicillin (100 U/mL) / streptomycin (100 µg/mL) (complete RPMI medium). The cytotoxicity of the tested molecules on the HepG2 (hepatocarcinoma cell line purchased from ATCC, ref HB-8065) cell line was assessed according to the method of Mosmann [45] with slight modifications. Briefly, 5.103 cells in 100 µL of complete medium were inoculated into each well of 96-well plates and incubated at 37 °C in humidified 5% $CO_2$. After 24 h incubation, 100 µL of medium with various product concentrations dissolved in DMSO (final concentration less than 0.5% v/v) were added and the plates were incubated for 72 h at 37 °C. Triplicate assays were performed for each sample. Each plate-well was then microscope examined for possible precipitate formation before the medium was aspirated from the wells. 100 µl of MTT (3-(4,5-dimethyl-2-thiazolyl)-2,5-diphenyl-2H-tetrazolium bromide) solution (0.5 mg/mL in medium without FBS) were then added to each well. Cells were incubated for 2 h at 37 °C. After this time, the

MTT solution was removed and DMSO (100 µL) was added to dissolve the resulting blue formazan crystals. Plates were shaken vigorously (700 rpm) for 10 min. The absorbance was measured at 570 nm with 630 nm as reference wavelength using a BIO-TEK ELx808 Absorbance Microplate Reader (LabX, Midland, ON, Canada). DMSO was used as blank and doxorubicin (purchased from Sigma Aldrich) as positive control. Cell viability was calculated as percentage of control (cells incubated without compound). The 50% cytotoxic concentration ($CC_{50}$) was determined from the dose–response curve, using TableCurve software 2D v.5.0. $CC_{50}$ values represent the mean value calculated from three independent experiments.

### 3.2.2. *In vitro* Cytotoxicity evaluation CHO

CHO cell line was maintained at 37 °C, 5% $CO_2$ with 90% humidity in RPMI supplemented with 10% foetal bovine serum, 1% L-glutamine (200 mM) and penicillin (100 U/mL) / streptomycin (100 µg/mL) (complete RPMI medium). The evaluation of the tested molecules cytotoxicity on the CHO cell line (purchased from ATCC, ref CCL-61) was performed according to the method of Mosmann with slight modifications. Briefly, $5.10^3$ cells in 100 µL of complete medium were inoculated into each well of 96-well plates and incubated at 37 °C in a humidified 5% $CO_2$. After 24 h incubation, 100 µL of medium with various product concentrations dissolved in DMSO (final concentration less than 0.5% v/v) were added and the plates were incubated for 24 h at 37 °C. Triplicate assays were performed for each sample. Each plate-well was then microscope-examined for detecting possible precipitate formation before the medium was aspirated from the wells. 100 µL of MTT (3-(4,5-dimethyl-2-thiazolyl)-2,5-diphenyl-2H-tetrazolium bromide) solution (0.5 mg/mL in medium without FCS) were then added to each well. Cells were incubated for 2 h at 37 °C. After this time, the MTT solution was removed and DMSO (100 µL) was added to dissolve the resulting blue formazan crystals. Plates were shaken vigorously (700 rpm) for 10 min. The absorbance was measured at 570 nm with 630 nm as reference wavelength using a BIO-TEK ELx808 Absorbance Microplate Reader. DMSO was used as blank and doxorubicin (purchased from Sigma Aldrich) as positive control. Cell viability was calculated as percentage of control (cells incubated without compound). The 50% cytotoxic concentration ($CC_{50}$) was determined from the dose–response curve by using the TableCurve software 2D v.5.0. $CC_{50}$ values represent the mean value calculated from three independent experiments.

### 3.2.3. *In vitro* Cytotoxicity evaluation VERO

VERO cell line was maintained at 37 °C, 5% $CO_2$ with 90% humidity in MEM supplemented with 10% foetal bovine serum, 1% L-glutamine (200 mM) and penicillin (100 U/mL) / streptomycin (100 µg/mL) (complete MEM medium). The evaluation of the tested molecules cytotoxicity on the VERO cell line (purchased from ATCC, ref CRL-1586) was performed according to the method of Mosmann with slight modifications. Briefly, $5.10^3$ cells in 100 µL of complete medium were inoculated into each well of 96-well plates and incubated at 37 °C in a humidified 5% $CO_2$. After 24 h incubation, 100 µL of medium with various product concentrations dissolved in DMSO (final concentration less than 0.5% v/v) were added and the plates were incubated for 48 h at 37 °C. Triplicate assays were performed for each sample. Each plate-well was then microscope-examined for detecting possible precipitate formation before the medium was aspirated from the wells. 100 µL of MTT (3-(4,5-dimethyl-2-thiazolyl)-2,5-diphenyl-2H-tetrazolium bromide) solution (0.5 mg/mL in medium without FCS) were then added to each well. Cells were incubated for 2 h at 37 °C. After this time, the MTT solution was removed and DMSO (100 µL) was added to dissolve the resulting blue formazan crystals. Plates were shaken vigorously (700 rpm) for 10 min. The absorbance was measured at 570 nm with 630 nm as

reference wavelength using a BIO-TEK ELx808 Absorbance Microplate Reader. DMSO was used as blank and doxorubicin (purchased from Sigma Aldrich) as positive control. Cell viability was calculated as percentage of control (cells incubated without compound). The 50% cytotoxic concentration ($CC_{50}$) was determined from the dose–response curve by using the TableCurve software 2D v.5.0. $CC_{50}$ values represent the mean value calculated from three independent experiments.

### 3.2.4. *In vitro* Antiplasmodial Evaluation

In this study, a K1 culture-adapted *P. falciparum* strain resistant to chloroquine, pyrimethamine, and proguanil was used in an in vitro culture. It was maintained in continuous culture as described previously by Trager and Jensen [46]. Cultures were maintained in fresh A+ human erythrocytes at 2.5% hematocrit in complete medium (RPMI 1640 with 25 mM HEPES, 25 mM $NaHCO_3$, 10% of A+ human serum) at 37 °C under reduced $O_2$ atmosphere (gas mixture 10% $O_2$, 5% $CO_2$, and 85% $N_2$). Parasitemia was maintained daily at between 1 and 3%. The *P. falciparum* drug susceptibility test was carried out by comparing quantities of DNA in treated and control cultures of parasite in human erythrocytes according to an SYBR Green I fluorescence-based method [47] using a 96-well fluorescence plate reader. Compounds, previously dissolved in DMSO (final concentration less than 0.5% *v*/*v*), were incubated in a total assay volume of 200 µL (RPMI, 2% hematocrit and 0.4% parasitemia) for 72 h in a humidified atmosphere (10% $O_2$ and 5% $CO_2$) at 37 °C, in 96-well flat bottom plates. Duplicate assays were performed for each sample. After incubation, plates were frozen at -20 °C for 24 h. Then, the frozen plates were thawed for 1 h at 37 °C. Fifteen µL of each sample were transferred to 96-well flat bottom non-sterile black plates (Greiner Bio-one) already containing 15 µL of the SYBR Green I lysis buffer (2X SYBR Green I, 20 mM Tris base pH 7.5, 20 mM EDTA, 0.008% w/v saponin, 0.08% w/v Triton X-100). Negative control treated by solvents (DMSO or $H_2O$) and positive controls (chloroquine and doxycycline) were added to each set of experiments. Plates were incubated for 15 min at 37 °C and then read on a TECAN Infinite F-200 spectrophotometer with excitation and emission wavelengths at 485 and 535 nm, respectively. The concentrations of compounds required to induce a 50% decrease of parasite growth ($EC_{50}$ K1) were calculated from three independent experiments.

### 3.2.5 Comet assay

#### 3.2.5.1. Cell culture and treatment

The human hepatocarcinoma cell line HepG2 was obtained from the American Type Culture Collection (ATCC, ref. HB-8065). Cells were cultured in Eagle's Minimum Essential Medium (EMEM, ref. ATCC® 30-2003TM) supplemented with 10% heat-inactivated foetal bovine serum, 100 U/mL penicillin and 0.1 mg/mL streptomycin (all from Gibco). Cells were maintained at 37 °C in a humidified atmosphere with 5% $CO_2$. Cells were used in passage number 11 to 15. Two concentrations of the compound **3k** (5.6 and 28 µM) were tested for 2 different times of incubation (2 and 72 h). Briefly, HepG2 cells were seeded at 1.13 x $10^5$ cells/mL in 6-well plates (3 mL of cell suspension per well) and incubated at 37 °C in a humidified atmosphere with 5% $CO_2$. After 24 and 94 h of incubation, cells were treated with different concentrations of the compound or the vehicle (0.5% dimethylsulfoxide, DMSO) for 72 and 2 h, respectively. Additionally, in the 2 h treatment plate, cells in an additional well were treated with 1 mM MMS as positive control for the comet assay. After treatment, medium was removed from the wells and cells were washed with phosphate buffered

saline (PBS). Finally, cells were trypsinized and trypsin was neutralized with fresh medium. From this point, cells were kept ice-cold to avoid DNA repair.

**3.2.5.2. Comet assay**

The standard alkaline comet assay was employed for the detection of DNA strand breaks (SBs) and alkali-labile sites (ALS) in cells treated with molecule **3k**. Trypsinized HepG2 cells were centrifuged at 125 g for 5 min at 4 °C and resuspended in cold PBS at 1 x $10^6$ cells/mL. For the preparation of the agarose gels, 30 µL of cell suspension were mixed with 140 µL of 1% low melting point agarose in PBS at 37 °C and 2 aliquots of 70 µL of cell/agarose mixture were placed on agarose-precoated microscope slides. Each droplet was covered with a 20 x 20 mm coverslip and after 2-3 min on a cold metal plate, the coverslips were removed. Then, slides were immersed in lysis solution (2.5 M NaCl, 0.1 M $Na_2EDTA$, 0.01 M Tris base, pH 10, and 1% Triton X-100) at 4 °C for 1 h. After lysis, slides were transferred to the electrophoresis tank and incubated for 40 min at 4 °C in the electrophoresis solution (0.3 M NaOH, 1 mM $Na_2EDTA$, pH > 13) to allow DNA unwinding. After that, electrophoresis was carried out at 1 V/cm for 20 min (4 °C). Then, gels were neutralized and washed by immersing the slides in PBS for 10 min and distilled water for another 10 min (both at 4 °C). Gels were then air dried at room temperature. Comets were stained by adding 30 µL of 1 mg/mL of 4,6- diamidino-2-phenylindole (DAPI) on top of each gel and placing 22 x 22 mm coverslips on top. Slides were incubated with DAPI at room temperature for 30 min before the analysis. The semiautomated image analysis system Comet Assay IV (Instem) was used to evaluate 50 comets per gel (i.e., 100/condition). The percentage of DNA in tail was the descriptor used for each comet.

**3.2.5.3. Statistics**

The median percentage of DNA in tail for 50 comets was calculated for each of the duplicate gels in each experiment, and the mean of the two medians was then calculated. The mean percentage of DNA in tail of 3 independent experiments and the standard deviation (SD) were calculated.

**3.2.6. APICOPLAST**

**3.2.6.1 Culturing *Plasmodium*-infected red blood cells**

*Plasmodium falciparum* blood stage parasites were maintained at 2% hematocrit in 1640 RPMI-HEPES supplemented with 5% AlbuMAX II (GIBCO) and 0.25% gentamycin. Parasites were grown sealed Perspex chambers gassed with beta mix gas (1% $O_2$, 5% $CO_2$ and 94% $N_2$) at 37 °C and maintained on 48-hour cycles. Cultures were tightly synchronized at ring stage using sorbitol treatment (5% v/v) as previously described [31].

**3.2.6.2 IFA on treated parasites**

Prior to the treatment parasites are synchronized using 5% sorbitol. After 48h treatment (0.3 µM of **(3k)** molecule, 0.3 µM of **(2a)** molecule or DMSO) parasites are fixed using 4% paraformaldehyde (PFA) and 0.0075% glutaraldehyde for 30 minutes at room temperature. Fixing solution is washed 3x times with PBS and cells are permeabilized with 0.1% TX-100 for 10 minutes at room temperature. Permeabilization solution is washed 3x times with PBS and cells are blocked with 3% fetal bovine serum (FBS) for 1 h. Primary antibody (Rat IgG anti-HA, Roche, 1/500 in 3% FBS) is incubated 1h at room temperature. Primary antibody is washed out 3x times with PBS and cells are incubated with secondary antibody (Alexa Fluor 488 goat anti-mouse IgG, Invitrogen, 1/1000 in 3% FBS) for 1h at room temperature. Secondary antibody is washed out 3x times with PBS and cells are incubated with

DAPI, 1/25000 in PBS. Samples are fixed between a slide and a coverslip with fluorogel and observed by epi-fluorescent microscopy.

**3.2.6.3 Growth assay**

To observe a potential effect of delayed death of the molecule on the parasite, *Plasmodium* is maintained on Three life cycles (48h). At 48 h, 96 h and 144 h, 100 µL of cultures are transferred into a 96 wells black wall flat bottom plate and mixed with 100 µL SYBR Green lysis buffer (20 mM Tris, pH 7.5; 5 mM EDTA; 0.008 % (w/v) saponin; 0.08% (v/v) Triton X-100) with freshly added SYBR Green I (10000X), and incubated 1h at room temperature protected from the light. Fluorescence from each well is measured with TECAN infinite M200 plate reader (excitation: 485 nm, emission: 538 nm and integration time: 1000 µs). The rest of the cultures are diluted 1/10 as the untreated cultures. Graph is obtain by doing the ration the treated culture fluorescence intensity on the untreated culture fluorescence intensity (n= 3).

**3.2.7. Study on the liver stage**

**3.2.7.1. Parasite strain and sporozoites isolation**

*P. falciparum* (NF135 strain) sporozoites were isolated by dissection of the salivary glands of infected *A. stephensi* 14-21 days after an infective blood meal (Department of medical microbiology, University Medical Centre, St Radboud, Nijmegen Netherland). All infected salivary glands were removed by hand dissection and crushed in a potter for sporozoites isolation and filtrated through a 40 µm filter to remove mosquito debris (Cell Strainer, BD BioSciences, USA). The sporozoites were counted using a disposable Glasstic microscope slide (KOVA, USA).

**3.2.7.2. Primary hepatocytes culture**

Conserved primary human hepatocytes were purchased from Biopredic International (France). Cells were seeded in 96-well plates (Falcon by Becton Dickinson Labware Europe, France) coated with collagen I (BD Biosience, USA), at a density of 80 000 cells per well. They are cultured at 37 °C in 5% $CO_2$ in William's E medium (Gibco, Life Technologies, Saint Aubin, France) supplemented with 10% of Foetal Bovine Serum FCIII, $5x10^{-5}$ M hydrocortisone hemisuccinate (Upjohn Laboratoires SERB, France), 5 µg per ml Insulin (Sigma Aldrich, USA), 2 mM L-glutamine, and 0.02 U per ml – 0.02 µg per ml penicillin – streptomycin (Life Technologies) until infection with sporozoites.

**3.2.7.3. *In vitro* infection and drug assays**

*P. falciparum* sporozoites were re-suspended in the above complete medium used for hepatocytes culture. Cultured human hepatocytes were inoculated with *P. falciparum* sporozoites (30,000 sporozoites/well of 96 well plates each) in 50 µl of complete media. The infected culture plate was centrifuged 10 min at 2000 rpm to allow fast parasite sedimentation onto the target cells and further incubated with serial dilution of drugs that were prepared in advance. After 3 hours incubation, cultures were washed and further incubated in fresh medium containing the appropriate drug concentration which were changed daily until cells fixation at day 6 post infection with 4%PFA for 20 min at room temperature.

The exo-erythrocytic forms (EEFs) were stained using the anti-HSP70 serum for *P. falciparum* and revealed with an Alexa 488-conjugated goat anti-mouse immunoglobulin (Molecular Probes). Host cell and parasite nuclei were labelled with 4',6-diamidino-2-phenylindole (DAPI). The EEFs were counted under a fluorescence microscope (Leica DMI4000B) or by using a CellInsight High Content Screening platform equipped with the Studio HCS software (Thermo Fisher, Scientific). To investigate the effect of drugs inhibition on the apicoplast maturation during liver-stage development, the EEFs

were stained using Acyl carrier protein (ACP) antibody and revealed with an Alexa Fluor 680-conjugated goat anti-rabbit immunoglobulin (Molecular Probes), and then imaged using a confocal microscope (Olympus FV1200). The images were analyzed using ImageJ software.

**3.2.7.4. Data analysis**

GraphPad Prism 7 statistical Software (GraphPad. Software, San Diego, CA, USA) were used for data analysis and graphing. All values were expressed as means and standard deviations (SD).

**References**


[1] World Health Organization (WHO), World Malaria Report 2020. Available online: URL https://www.who.int/publications-detail-redirect/world-malaria-report-2020 (accessed 08 January 2021).

[2] Trape J. F. The public health impact of chloroquine resistance in Africa. *Am. J. Trop. Med. Hyg*. **2001**, *64*, 12-17, doi.org/10.4269/ajtmh.2001.64.12.

[3] Veiga, M I.; Dhingra1, SK.; Henrich, P P.; Straimer, J.; Gna¨dig, N. ; Uhlemann, A-C.; Martin, R E.; Lehane, A M.; Fidock, D A.Globally prevalent PfMDR1 mutations modulate *Plasmodium falciparum* susceptibility to artemisinin-based combination therapies. *Nature Commun.* **2016**, 7:11553, doi.org/10.1038/ncomms11553.

[4] Vaidya, A. B.; Mather, M. W. Atovaquone Resistance in Malaria Parasites. *Drug Resist. Updat.* **2000**, *3*, 283-287, doi.org/10.1054/drup.2000.0157.

[5] Uhlemann, A. C.; Krishna, S. Antimalarial multi-drug resistance in Asia: mechanisms and assessment. *Curr. Top. Microbiol. Immunol*. **2005**, *295*, 39-53, doi.org/10.1007/3-540-29088-5_2.

[6] Eastman, R. T.; Dharia, N. V.; Winzeler, E. A.; Fidock, D. A. Piperaquine Resistance Is Associated with a Copy Number Variation on Chromosome 5 in Drug-Pressured *Plasmodium falciparum* Parasites. *Antimicrob. Agents Chemother.* **2011**, *55*, 3908–3916. doi.org/10.1128/AAC.01793-10.

[7] Plowe, C. V. Monitoring Antimalarial Drug Resistance: Making the Most of the Tools at Hand. *J. Exp. Biol.* **2003**, *206*, 3745–3752. doi.org/10.1242/jeb.00658.

[8] Sibley, C. H.; Hyde, J. E.; Sims, P. F.; Plowe, C. V.; Kublin, J. G.; Mberu, E. K.; Cowman, A. F.; Winstanley, P. A.; Watkins, W. M.; Nzila, A. M. Pyrimethamine-Sulfadoxine Resistance in Plasmodium Falciparum: What Next? *Trends Parasitol.* **2001**, *17*, 582–588. doi.org/10.1016/s1471-4922(01)02085-2

[9] Menard, D.; Dondorp, A. Antimalarial Drug Resistance: A Threat to Malaria Elimination. *Cold. Spring. Harb. Perspect. Med.* **2017**, *7*:a025619, doi.org/10.1101/cshperspect.a025619.

[10] Lu, F.; Culleton, R.; Zhang, M.; Ramaprasad, A.; von Seidlein, L.; Zhou, H.; Zhu, G.; Tang, J.; Liu, Y.; Wang, W.; Cao, Y.; Xu, S.; Gu, Y.; Li, J.; Zhang, C.; Gao, Q.; Menard, D.; Pain, A.; Yang, H.; Zhang, Q.; Cao, J. Emergence of Indigenous Artemisinin-Resistant Plasmodium Falciparum in Africa. *N. Engl. J. Med.* **2017**, *376*, 991–993, doi.org/10.1056/NEJMc1612765.

[11] Uwimana, A.; Legrand, E.; Stokes, B. H.; Ndikumana, J.-L. M.; Warsame, M.; Umulisa, N.; Ngamije, D.; Munyaneza, T.; Mazarati, J.-B.; Munguti, K.; Campagne, P.; Criscuolo, A.; Ariey, F.; Murindahabi, M.; Ringwald, P.; Fidock, D. A.; Mbituyumuremyi, A.; Menard, D. Emergence and Clonal

Expansion of in Vitro Artemisinin-Resistant Plasmodium Falciparum Kelch13 R561H Mutant Parasites in Rwanda. *Nat. Med.* **2020**, *26*, 1602–1608, doi.org/10.1038/s41591-020-1005-2.

[12] Rosenthal, P. J. Artemisinin Resistance in Eastern India. *Clin. Infect. Dis.* **2019**, *69*, 1153–1155, doi.org/10.1093/cid/ciy1043.

[13] Verhaeghe, P.; Rathelot, P.; Rault, S.; Vanelle, P. Convenient Preparation of Original Vinylic Chlorides with Antiparasitic Potential in Quinoline Series. *Lett. Org. Chem.* **2006**, *3*, 891-897. doi.org/10.2174/157017806779467997

[14] Primas, N.; Verhaeghe, P.; Cohen, A.; Kieffer, C.; Dumètre, A.; Hutter, S.; Rault, S.; Rathelot, P.; Azas, N.; Vanelle, P. A New Synthetic Route to Original Sulfonamide Derivatives in 2-Trichloromethylquinazoline Series: A Structure-Activity Relationship Study of Antiplasmodial Activity. *Molecules* **2012**, *17*, 8105–8117, doi.org/10.3390/molecules17078105.

[15] Gellis, A.; Kieffer, C.; Primas, N.; Lanzada, G.; Giorgi, M.; Verhaeghe, P.; Vanelle, P. A New DMAP-Catalyzed and Microwave-Assisted Approach for Introducing Heteroarylamino Substituents at Position 4 of the Quinazoline Ring. *Tetrahedron* **2014**, *78*, 8257–8266, doi.org/10.1016/j.tet.2014.09.024.

[16] Verhaeghe, P.; Dumètre, A.; Castera-ducros, C.; Hutter, S.; Laget, M.; Fersing, C.; Prieri, M.; Yzombard, J.; Sifredi, F.; Rault, S.; Rathelot, P.; Vanelle, P.; Azas, N. 4-Thiophenoxy-2-Trichloromethyquinazolines Display in Vitro Selective Antiplasmodial Activity against the Human Malaria Parasite *Plasmodium falciparum*. *Bioorg. Med. Chem. Lett.* **2011**, *21*, 6003–6006, doi.org/10.1016/j.bmcl.2011.06.113.

[17] Desroches, J.; Kieffer, C.; Primas, N.; Hutter, S.; Gellis, A.; El-Kashef, H.; Rathelot, P.; Verhaeghe, P.; Azas, N.; Vanelle, P. Discovery of New Hit-Molecules Targeting Plasmodium Falciparum through a Global SAR Study of the 4-Substituted-2-Trichloromethylquinazoline Antiplasmodial Scaffold. *Eur. J. Med. Chem.* **2017**, *125*, 68–86, doi.org/10.1016/j.ejmech.2016.09.029.

[18] McNamara, C. W.; Lee, M. C. S.; Lim, C. S.; Lim, S. H.; Roland, J.; Nagle, A.; Simon, O.; Yeung, B. K. S.; Chatterjee, A. K.; McCormack, S. L.; Manary, M. J.; Zeeman, A.-M.; Dechering, K. J.; Kumar, T. R. S.; Henrich, P. P.; Gagaring, K.; Ibanez, M.; Kato, N.; Kuhen, K. L.; Fischli, C.; Rottmann, M.; Plouffe, D. M.; Bursulaya, B.; Meister, S.; Rameh, L.; Trappe, J.; Haasen, D.; Timmerman, M.; Sauerwein, R. W.; Suwanarusk, R.; Russell, B.; Renia, L.; Nosten, F.; Tully, D. C.; Kocken, C. H. M.; Glynne, R. J.; Bodenreider, C.; Fidock, D. A.; Diagana, T. T.; Winzeler, E. A. Targeting Plasmodium PI(4)K to Eliminate Malaria. *Nature* **2013**, *504*, 248–253, doi.org/10.1038/nature12782.

[19] Guillon, J.; Cohen, A.; Gueddouda, N. M.; Das, R. N.; Moreau, S.; Ronga, L.; Savrimoutou, S.; Basmaciyan, L.; Monnier, A.; Monget, M.; Rubio, S.; Garnerin, T.; Azas, N.; Mergny, J.-L.; Mullié, C.; Sonnet, P. Design, Synthesis and Antimalarial Activity of Novel Bis *N*-[(Pyrrolo[1,2-a]Quinoxalin-4-Yl)Benzyl]-3-Aminopropylamine Derivatives. *J. Enzyme Inhib. Med. Chem.* **2017**, *32*, 547–563. doi.org/10.1080/14756366.2016.1268608.

[20] Jonet, A.; Guillon, J.; Mullie, C.; Cohen, A.; Bentzinger, G.; Schneider, J.; Taudon, N.; Hutter, S.; Azas, N.; Moreau, S.; Savrimoutou, S.; Agnamey, P.; Dassonville-Klimpt, A.; Sonnet, P. Synthesis and Antimalarial Activity of New Enantiopure Aminoalcoholpyrrolo[1,2-*a*]quinoxalines. *Med. Chem.* **2018**, *14*, 293-303. doi.org/10.2174/1573406413666170726123938.

[21] Primas, N.; Suzanne, P.; Verhaeghe, P.; Cohen, A.; Broggi, J.; Lancelot, J.; Kieffer, C.; Vanelle, P.; Azas, N. Synthesis and in Vitro Evaluation of 4-Trichloromethylpyrrolo [1,2-*a*] Quinoxalines as New Antiplasmodial Agents. *Eur. J. Med. Chem.* **2014**, *83*, 26–35. doi.org/10.1016/j.ejmech.2014.06.014.

[22] Burrows, J. N.; Duparc, S.; Gutteridge, W. E.; Huijsduijnen, R. H. Van; Kaszubska, W.; Macintyre, F.; Mazzuri, S.; Möhrle, J. J.; Wells, T. N. C. New Developments in Anti-Malarial Target Candidate and Product Profiles. *Malar. J.* **2017**, 16:26, doi.org/10.1186/s12936-016-1675-x.

[23] MMV-supported projects | Medicines for Malaria Venture https://www.mmv.org/research-development/mmv-supported-projects (accessed Feb 21, 2021)

[24] Weatherby, K.; Carter, D. *Chromera velia*: The Missing Link in the Evolution of Parasitism. *Adv. Appl. Microbiol.* **2013**, *85*, 119–144. doi.org/10.1016/B978-0-12-407672-3.00004-6.

[25] McFadden, G. I.; Yeh, E. The Apicoplast: Now You See It, Now You Don't. *Int. J. Parasitol.* **2017**, *47*, 137–144. doi.org/10.1016/j.ijpara.2016.08.005.

[26] Botté, C. Y.; Dubar, F.; McFadden, G. I.; Maréchal, E.; Biot, C. *Plasmodium falciparum* Apicoplast Drugs: Targets or off-Targets? *Chem. Rev.* **2012**, *112*, 1269–1283. doi.org/10.1021/cr200258w.

[27] Mukherjee, A.; Sadhukhan, G. C. Anti-Malarial Drug Design by Targeting Apicoplasts: New Perspectives. *J. Pharmacopuncture* **2016**, *19*, 7–15. doi.org/10.3831/KPI.2016.19.001.

[28] Uddin, T.; McFadden, G. I.; Goodman, C. D. Validation of Putative Apicoplast-Targeting Drugs Using a Chemical Supplementation Assay in Cultured Human Malaria Parasites. *Antimicrob. Agents Chemother.* **2018**, 62:e01161-17. doi.org/10.1128/AAC.01161-17.

[29] Vaughan, A. M.; O'Neill, M. T.; Tarun, A. S.; Camargo, N.; Phuong, T. M.; Aly, A. S. I.; Cowman, A. F.; Kappe, S. H. I. Type II Fatty Acid Synthesis Is Essential Only for Malaria Parasite Late Liver Stage Development. *Cell. Microbiol.* **2009**, *11* , 506–520. doi.org/10.1111/j.1462-5822.2008.01270.x.

[30] Botté, C. Y.; Yamaryo-Botté, Y.; Rupasinghe, T. W. T.; Mullin, K. A.; MacRae, J. I.; Spurck, T. P.; Kalanon, M.; Shears, M. J.; Coppel, R. L.; Crellin, P. K.; Maréchal, E.; McConville, M. J.; McFadden, G. I. Atypical Lipid Composition in the Purified Relict Plastid (Apicoplast) of Malaria Parasites. *PNAS* **2013**, *110*, 7506–7511, doi.org/10.1073/pnas.1301251110.

[31] Amiar, S.; Katris, N. J.; Berry, L.; Dass, S.; Duley, S.; Arnold, C.-S.; Shears, M. J.; Brunet, C.; Touquet, B.; McFadden, G. I.; Yamaryo-Botté, Y.; Botté, C. Y. Division and Adaptation to Host Environment of Apicomplexan Parasites Depend on Apicoplast Lipid Metabolic Plasticity and Host Organelle Remodeling. *Cell Reports* **2020**, *30*, 3778-3792, doi.org/10.1016/j.celrep.2020.02.072.

[32] Swift, R. P.; Rajaram, K.; Liu, H. B.; Prigge, S. T. Dephospho-CoA Kinase, a Nuclear-Encoded Apicoplast Protein, Remains Active and Essential after Plasmodium Falciparum Apicoplast Disruption. *The EMBO Journal* **2021**, e107247, doi.org/10.15252/embj.2020107247.

[33] Swift, R. P.; Rajaram, K.; Keutcha, C.; Liu, H. B.; Kwan, B.; Dziedzic, A.; Jedlicka, A. E.; Prigge, S. T. The NTP Generating Activity of Pyruvate Kinase II Is Critical for Apicoplast Maintenance in Plasmodium Falciparum. *eLife* **2020**, *9*, e50807. doi.org/10.7554/eLife.50807.

[34] Ghavami, M.; Merino, E. F.; Yao, Z.-K.; Elahi, R.; Simpson, M. E.; Fernández-Murga, M. L.; Butler, J. H.; Casasanta, M. A.; Krai, P. M.; Totrov, M. M.; Slade, D. J.; Carlier, P. R.; Cassera, M. B. Biological Studies and Target Engagement of the 2-C-Methyl-d-Erythritol 4-Phosphate Cytidylyltransferase

(IspD)-Targeting Antimalarial Agent (1R,3S)-MMV008138 and Analogs. *ACS Infect. Dis.* **2018**, *4*, 549–559. doi.org/10.1021/acsinfecdis.7b00159.

[35] Baschong, W.; Wittlin, S.; Inglis, K. A.; Fairlamb, A. H.; Croft, S. L.; Kumar, T. R. S.; Fidock, D. A.; Brun, R. Triclosan Is Minimally Effective in Rodent Malaria Models. *Nat. Med.* **2011**, *17*, 33–34. https://doi.org/10.1038/nm0111-33.

[36] Witschel, M.; Rottmann, M.; Kaiser, M.; Brun, R. Agrochemicals against Malaria, Sleeping Sickness, Leishmaniasis and Chagas Disease. *PLOS Negl. Trop. Dis.* **2012**, *6*, e1805. doi.org/10.1371/journal.pntd.0001805.

[37] Corral, M. G.; Leroux, J.; Stubbs, K. A.; Mylne, J. S. Herbicidal Properties of Antimalarial Drugs. *Sci. Rep.* **2017**, *7*, 45871. doi.org/10.1038/srep45871.

[38] Clastre, M.; Goubard, A.; Prel, A.; Mincheva, Z.; Viaud-Massuart, M.-C.; Bout, D.; Rideau, M.; Velge-Roussel, F.; Laurent, F. The Methylerythritol Phosphate Pathway for Isoprenoid Biosynthesis in Coccidia: Presence and Sensitivity to Fosmidomycin. *Exp. Parasitol.* **2007**, *116*, 375–384. doi.org/10.1016/j.exppara.2007.02.002.

[39] Nagamune, K.; Hicks, L. M.; Fux, B.; Brossier, F.; Chini, E. N.; Sibley, L. D. Abscisic Acid Controls Calcium-Dependent Egress and Development in *Toxoplasma Gondii*. *Nature* **2008**, *451*, 207–210. doi.org/10.1038/nature06478.

[40] Verhaeghe, P.; Rathelot, P.; Gellis, A.; Vanelle, P. Highly Efficient Microwave Assisted a -Trichlorination Reaction of a -Methylated Nitrogen Containing Heterocycles. *Tetrahedron* **2006**, *62*, 8173–8176. doi.org/10.1016/j.tet.2006.05.081

[41] Amrane, D.; Gellis, A.; Hutter, S.; Prieri, M.; Verhaeghe, P.; Azas, N.; Vanelle, P.; Primas, N. Synthesis and Antiplasmodial Evaluation of 4-Carboxamido- and 4-Alkoxy-2-Trichloromethyl Quinazolines. *Molecules* **2020**, *25*, 3929. doi.org/10.3390/molecules25173929.

[42] Stumpfe, D.; Bajorath, J. Exploring Activity Cliffs in Medicinal Chemistry. *J. Med. Chem.* **2012**, *55*, 2932–2942. doi.org/10.1021/jm201706b.

[43] Wagle, S.; Adhikari, A. V.; Kumari, N. S. Synthesis of Some New 4-Styryltetrazolo[1,5-a]Quinoxaline and 1-Substituted-4-Styryl[1,2,4]Triazolo[4,3-a]Quinoxaline Derivatives as Potent Anticonvulsants. *Eur J. Med. Chem.* **2009**, *44*, 1135–1143. doi.org/10.1016/j.ejmech.2008.06.006.

[44] Wei, Z.; Qi, S.; Xu, Y.; Liu, H.; Wu, J.; Li, H.; Xia, C.; Duan, G. Visible Light-Induced Photocatalytic C−H Perfluoroalkylation of Quinoxalinones under Aerobic Oxidation Condition. *Adv. Synth. Catal.* **2019**, *361*, 5490–5498. doi.org/10.1002/adsc.201900885

[45] Mosmann, T. Rapid Colorimetric Assay for Cellular Growth and Survival: Application to Proliferation and Cytotoxicity Assays. *J. Immunol. Methods* **1983**, *65*, 55–63. doi.org/10.1016/0022-1759(83)90303-4.

[46] Trager, W.; Jensen, J. B. Human Malaria Parasites in Continuous Culture. *Science* **1976**, *193*, 673–675. doi.org/10.1126/science.781840.

[47] Guiguemde, W. A.; Shelat, A. A.; Bouck, D.; Duffy, S.; Crowther, G. J.; Davis, P. H.; Smithson, D. C.; Connelly, M.; Clark, J.; Zhu, F.; Jiménez-Díaz, M. B.; Martinez, M. S.; Wilson, E. B.; Tripathi, A. K.; Gut, J.; Sharlow, E. R.; Bathurst, I.; El Mazouni, F.; Fowble, J. W.; Forquer, I.; McGinley, P. L.; Castro, S.;

1076 Angulo-Barturen, I.; Ferrer, S.; Rosenthal, P. J.; Derisi, J. L.; Sullivan, D. J.; Lazo, J. S.; Roos, D. S.;
1077 Riscoe, M. K.; Phillips, M. A.; Rathod, P. K.; Van Voorhis, W. C.; Avery, V. M.; Guy, R. K. Chemical
1078 Genetics of *Plasmodium falciparum*. *Nature* **2010**, *465*, 311–315. doi.org/10.1038/nature09099.